18L

PNL-4743
UC-94e

Reservoir Characterization and Final Pre-Test Analysis in Support of the Compressed Air Energy Storage Pittsfield Aquifer Field Test in Pike County, Illinois

L. E. Wiles
R. A. McCann

June1983

Prepared for the U.S. Department of Energy
under Contract DE-AC06-76RLO 1830

Pacific Northwest Laboratory
Operated for the U.S. Department of Energy
by Battelle Memorial Institute

Battelle

PNL-4743

DISCLAIMER

PACIFIC NORTHWEST LABORATORY
operated by
BATTELLE
for the
UNITED STATES DEPARTMENT OF ENERGY
under Contract *DE-AC06-76RLO* ***7830***

Printed in the United States of America
Available from
National Technical Information Service
United States Department of Commerce
5285 Port Royal Road
Springfield, Virginia 22161

NTIS **Price Codes** A04
Microfiche A01

Printed Copy

Pages	Price Codes
001-025	A02
026-050	A03
051-075	A04
076-100	A05
101-125	A06
126-150	A07
151-175	A08
176-200	A09
201-225	A010
226-250	A011
251-275	A012
276-300	A013

PNL-4743
UC-94e

RESERVOIR CHARACTERIZATION AND FINAL PRE-TEST ANALYSIS IN SUPPORT OF THE COMPRESSED AIR ENERGY STORAGE PITTSFIELD AQUIFER FIELD TEST IN PIKE COUNTY, ILLINOIS

L. E. Wiles
R. A. McCann

June 1983

Prepared for
the U.S. Department of Energy
under Contract DE-AC06-76RLO 1830

Pacific Northwest Laboratory
Richland, Washington 99352

FOREWORD

Compressed air energy storage (CAES) is a technique that transfers energy from off-peak to peak demand time for electric utility systems. It incorporates modified state-of-the-art gas turbines and underground reservoirs--aquifers, salt cavities, or mined hard rock caverns. The compressor and turbine sections of the gas turbine are alternately coupled to a motor/generator for operation during different time periods. During off-peak electric demand periods, base load plants not using petroleum fuels provide energy to compress air, which is stored in the underground reservoirs. During peak-load electric demand periods, the compressed air is withdrawn from storage, mixed with fuel, combusted and then expanded through the turbines to generate electricity. Because the turbine is not required to drive a compressor, this concept reduces peaking plant consumption of petroleum fuel by more than 60%.

Since 1975, the Pacific Northwest Laboratory (PNL) has served as the U.S. Department of Energy's lead laboratory in managing research and development efforts to support CAES technology commercialization.

A substantial part of the CAES Technology Projects is represented by the Reservoir Stability Studies. The goal of these studies is to ensure long-term stable containment of air in the underground reservoirs used in conjunction with CAES plants. The specific objective is to develop stability criteria and engineering guidelines for designing CAES reservoirs in each of the three major reservoir types, including aquifers, salt cavities, and mined hard rock caverns.

Three parallel studies have been performed. Each contained a survey of the state-of-the-art and numerical and experimental studies. The mined hard rock and salt studies were completed and final criteria documents have been issued. The aquifer study has also been completed as a generic study, but has been extended to include a specific field experiment, the Pittsfield Aquifer Test.

The objective of this document is to demonstrate numerical computer modeling capabilities developed during previous comprehensive research projects. Analysis was performed in support of the design, construction and operation of the Pittsfield Aquifer Field Test. The computer models developed at PNL were used to examine pressure response, bubble development, water coning, thermal development, and dehydration processes.

Modeling was applied to the field test to assist in system design and equipment selection, to aid in baseline test planning and to predict test performance. Once testing was underway, modeling was used for performance matching, which assisted in the interpretation of reservoir response and allowed problem diagnosis in conjunction with the limited available instrumentation. The results of these analyses demonstrate that modeling can be a tremendous asset in understanding the response of the Pittsfield Aquifer Test reservoir.

There have been differences between anticipated performance and actual performance of the Pittsfield Aquifer Test. Careful study in the future is necessary to interpret whether these variations are attributable to construction variations, incomplete reservoir characteristics or modeling assumptions and formulations. This work is presented to provide a baseline from which such later studies can proceed.

The information presented herein is being used, in conjunction with results of actual field tests and other data, as the basis for the porous media reservoir stability criteria. An interim version of this criteria and guidelines document (PNL-4707) was issued by PNL in May 1983.

T. J. Doherty
Compressed Air Energy Storage Project
Pacific Northwest Laboratory

SUMMARY

Pacific Northwest Laboratory (PNL) initiated a field test program under sponsorship of the U.S. Department of Energy to evaluate compressed air energy storage (CAES) in a porous media aquifer reservoir. The field test site is near Pittsfield, Illinois. A numerical modeling analysis performed in support of the field test defined the reservoir's anticipated thermohydraulic performance based upon a reservoir description representing the most current data available. A final pre-test analysis was also conducted.

The three primary objectives of the numerical analysis were to assess the specification of instrumentation and above-ground equipment, to define the time required to develop an adequately sized air storage bubble, and to develop and evaluate operational strategies for air cycling. The principal concerns involved with the air cycling phase of the field test are the potential for water production and the thermal development. This document describes the parametric analysis performed to meet these objectives for the field test reservoir.

Analysis was performed with a series of finite difference computer codes written during previous stages of the porous media reservoir studies. These codes have the capability to characterize pressure and temperature response, to characterize near-wellbore desaturation by phase change, and to simulate the displacement of water by air within the porous medium.

The findings of the numerical analysis led to several primary conclusions:

The air compressor is sufficient to develop an air storage bubble of adequate size for testing in 2 to 3 months.

- Operational controls in conjunction with a low vertical permeability in the reservoir appear sufficient to significantly reduce the potential for water production.

- A mass- and pressure-balanced cycle is recommended. For a reservoir of 700 md horizontal permeability and 135 md vertical permeability, this would consist of about 7 hr of air injection at 1250 scfm, 11 hr of air withdrawal at 795 scfm, and 6 hr of reservoir closure, with reservoir closure on weekends.
- Field test duration is sufficient to evaluate the thermal performance at the instrumented observation wells.

Some data is available at the time of this publication on bubble development operations at the Pittsfield Aquifer Test. This data indicates that reservoir injection/withdrawal rates and pressures vary significantly from the anticipated performance as outlined within this document. Preliminary review points to near-well restrictions not accounted for in these analyses. Care should be taken in interpreting field study results directly against the conclusions of this work, as a number of factors such as operational strategy, the level of reservoir characterization, construction flaws and well completion details can account for significant differences between specific factors. It must be remembered that the purposes of the modeling are to 1) delineate and evaluate, through parametric analysis, the factors that will significantly affect system behavior and 2) provide a specific baseline from which one can interpret actual system performance, along with a set of rational methods that are useful in that interpretation.

Previous documents on model development and parametric analysis have provided an understanding of the primary mechanisms operating in aquifer air storage systems. This document is intended to provide a basis for understanding and interpreting the results of the Pittsfield Aquifer Test.

CONTENTS

FIGURES

TABLE

RESERVOIR CHARACTERIZATION AND FINAL PRE-TEST ANALYSIS IN SUPPORT OF THE COMPRESSED AIR ENERGY STORAGE PITTSFIELD AQUIFER FIELD TEST IN PIKE COUNTY, ILLINOIS

1.0 INTRODUCTION

Pacific Northwest Laboratory (PNL) initiated a field experimental program in 1981 under sponsorship of the U.S. Department of Energy to demonstrate and evaluate compressed air energy storage (CAES) in a porous media aquifer reservoir. The site of the field test is near Pittsfield, Illinois. The air injection zone is composed of the St. Peter sandstone. The storage formation is at a depth of 200 m and is overlain by dolomitic and limestone caprock of sufficient thickness and low permeability to contain air. The closure is obtained within a second-order dome, one of several known minor structures associated with the Pittsfield anticline. The field test site was developed with a single injection/withdrawal well. Two instrumented observation wells were located at 2 and 8 m from the injection/withdrawal well. Several observation wells were placed at various radial azimuths between 100 and 300 m from the injection/withdrawal well.

Numerical modeling of the Pittsfield reservoir was performed concurrently with site development. The numerical models, developed at PNL for the CAES program, were applied to predict the thermohydraulic performance of the porous media reservoir. This reservoir characterization and pre-test analysis made use of our ability to evaluate four distinct problems: bubble development, water coning, thermal development, and near-wellbore desaturation.

Initially, the reservoir is fully saturated with liquid water. During bubble development, air is injected continuously into the reservoir, gradually displacing the aquifer water. The displacement front is not sharp, however. As the saturation approaches the residual, or irreducible,

value, the liquid mobility approaches zero and this water is retained within the rock structure. In addition, capillary forces tend to retain water within the bubble in a region called the transition zone, located between the fully saturated zone and the region of residual water content. Because of its small vertical thickness, the Pittsfield reservoir air storage zone may be dominated by the transition zone. This means that mobile water may surround the wellbore during bubble development and, as air cycling begins, this could result in reduced air flow or some water production. This type of water production may be insignificant, particularly if any near-wellbore desaturation has occurred during bubble development due to the injection of undersaturated air.

Water production due to water coning could have more serious impacts on the field test. Water coning occurs as air is withdrawn from the reservoir. Water below the wellbore responds to the same pressure gradients that drive the air from the reservoir. The water rises as air is withdrawn and the water recedes during the subsequent injection of air. However, if an imbalance exists between the combined effects of cycle length, the pressure gradients or the liquid mobilities on either side of the injection/withdrawal cycle, then net water migration toward the wellbore can occur. If the pressure gradients are strong enough and/or exist long enough, eventual water production could occur. This would be indicated by an increasing degradation of air flow at a constant back pressure.

Continuous water production could also cause chemical degradation of the sandstone around the wellbore and result in eventual pore plugging, particularly in conjunction with thermal development. These geochemical processes will occur at much higher rates as temperature is increased. Thermal cycling may also cause degradation of material properties. Although thermal development may introduce these problems, it also offers certain potential benefits. Thermal development can be used to effect thermal energy storage in the reservoir. Eventually, the temperature of air withdrawn from the reservoir approaches the temperature of the injected

air. Near-wellbore desaturation due to phase change actually has a minimal effect on these temperatures. This desaturation will have the benefit of eliminating water from the high temperature zone of the reservoir, thereby reducing the potential for adverse geochemical reactions to affect reservoir performance.

The work reported here was undertaken

- to define the time required to develop an air storage bubble of adequate size
- to assess the specification of instrumentation and above-ground equipment
- to develop and evaluate operational strategies for air cycling.

As a result of the work to characterize the expected performance of the reservoir, a parametric analysis was performed for the field test reservoir. If the reservoir does not perform according to the predictions, then a basis will exist for changing the reservoir description. This will be done in such a way that the description of the reservoir is more accurate, making subsequent model predictions more accurate.

Pre-test analyses determined that the horizontal permeability has a significantly greater impact on the bubble development than does the vertical permeability. It appears that operational controls may not be sufficient to preclude eventual water production without causing adverse impacts on other aspects of the field test. It was verified that the air compressor is of adequate size to develop the air bubble in 60 to 75 days. The air drier provides an injection humidity sufficiently close to zero. The humidity measurement system for the withdrawal air flow was designed to measure a range of values predicted with the models. Instrumentation to measure pressure, temperature, humidity, and saturation, both at the surface and down hole, was specified from model predictions. Expected drawdown pressure and bottomhole injection pressures were defined. An injection/withdrawal schedule was defined, which apparently avoids water

coning based on core data indicating some low vertical permeabilities. The basic test plan for the actual field test was developed on the basis of the analysis.

This report presents the analysis and results leading to the characterization of reservoir performance. This final pre-test analysis uses the most current reservoir data. Conclusions based on this analysis are presented in Section 2.0. The Pittsfield reservoir is described in Section 3.0. In Section 4.0, the numerical models used in this analysis are described. Section 5.0 discusses the reservoir characterization. The final pre-test analysis is presented in Section 6.0. Descriptions of future related work are outlined in Section 7.0.

2.0 CONCLUSIONS

The primary conclusions of the reservoir characterization and pre-test analysis in support of the CAES porous media field test at Pittsfield are as follows:

- The air compressor should be of adequate size to develop the air storage bubble in 60 to 75 days.
- The air bubble growth rate is directly a function of horizontal permeability and is almost independent of vertical permeability.
- The only operational control effective at reducing the potential for water production is a skewed cycle in which air is withdrawn at a low flow rate to reduce the pressure gradient that drives water toward the wellbore.
- Operational controls in conjunction with a low vertical permeability in the reservoir apparently are sufficient to significantly reduce the potential for water production.
- A mass- and pressure-balanced cycle is recommended. For a reservoir of 700 md horizontal permeability and 135 md vertical permeability, this would consist of approximately 7 hr of air injection at 1250 scfm, 11 hr of air withdrawal at 795 scfm, and 6 hr of reservoir closure, with reservoir closure on the weekends.

  The duration of the field test should be sufficient to obtain a measurable thermal response at the instrumented observation wells, thereby providing data for evaluation of the thermal performance of the reservoir.

3.0 RESERVOIR DESCRIPTION

The site of the field test is near Pittsfield, Illinois. The air injection zone is composed of the St. Peter sandstone. The St. Peter formation is at a depth of about 200 m and is overlain by dolomitic and limestone caprock of sufficient thickness and low permeability to contain air. The closure is obtained within a second-order dome, one of several known minor structures associated with the Pittsfield anticline. A general description of the reservoir structure and geometry, as well as material properties, was defined from exploratory drilling, field logs, and laboratory analysis of core samples. This data was used to develop a reservoir description that was acceptable for numerical analysis. That is, locally averaged data is required for the finite difference analysis. For example, although permeability may vary by orders of magnitude within a given zone, some averaged value must be applied to the computational cell representing that zone. In addition, some site-specific data was not available. For example, the thermal properties and the saturation functions were merely typical of St. Peter sandstone. The conditions that were actually applied in the analysis are discussed here and summarized in Table 3.1. Excluding variations of properties for parametric study, the assigned values of properties represented our best knowledge of the Pittsfield reservoir prior to the initiation of air injection.

For the numerical analysis, the reservoir is idealized as an axisymmetric region as shown in Figure 3.1. The injection/withdrawal (I/W) well is at the center where the vertical thickness of the storage zone is 68 m. The producing section of the I/W well extends 2.7 m from the bottom of the caprock. The caprock has a uniform slope of 1/80. The basement rock is uniform with zero slope.

The radius to the sandface in the wellbore is 10 cm. The outer radius of the computational region is 760 m. The radius to a hydrostatic sink is defined as 10,000 m. This "hydrostatic radius" is an assumed value that acts as a boundary condition for the flow of water through the outer

TABLE 3.1. Reservoir Description

Geometry	
Depth to top of structure	215 m
Caprock slope	1/80
Vertical thickness of storage zone	68 m
Well diameter	20 cm
Producing length	2.7 m
Outer radius of modeled region	760 m
Assumed radius to hydrostatic pressure	10^4 m
Properties	
Permeability (horizontal)	700 md
(vertical)	700 md
Porosity	20%
Rock thermal conductivity	2.16 W/m°C
Rock thermal capacity	2.62 MJ/m^3°C
Saturation functions	
Relative permeability	
(air) $k_r^g = \left(S_{c,g} - S\right)^2 \left[2.34 - 1.37\left(Sc,g - S\right)^2\right]$	
(water) $k_r^\ell = (S - Sc,\ell)^3 \left[4.93 - 3.72\left(S - S_{c,\ell}\right)\right]$	
where S is the porous media saturation (i.e., ratio of pore water volume to total pore volume)	
Critical saturation for gas mobility,	$S_{c,g} = 0.90$
Critical saturation for liquid mobility,	$S_{c,\ell} = 0.20$
Capillary pressure $P_c = \left(\frac{0.05525}{S-0.15}\right) - 0.065$ atm	
Operating conditions	
Discovery pressure	10 atm
Maximum injection pressure	18.7 atm
Maximum injection air flow rate	1250 scfm
Discovery temperature	14°C
Maximum injection temperature	200°C
Injection humidity	0
Air viscosity $[0.608 \times 10^{-4} + 0.4 \times 10^{-6}\ (°K)]$ gm/cm·sec	

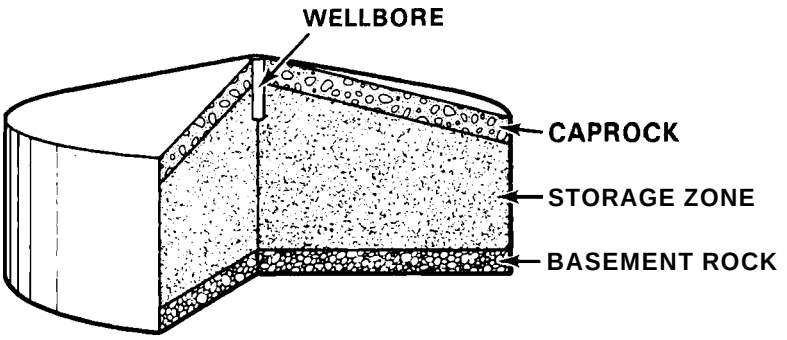

FIGURE 3.1. Reservoir Structure

radius of the computational region. The hydrostatic radius is the distance from the I/W well to a point where the pressure remains constant at its hydrostatic value. Performance data from the field test will be necessary to adjust the hydrostatic radius and to improve the description of the interaction between the air storage zone and the surrounding aquifer.

Much of the analysis was performed using a homogeneous, isotropic permeability of 700 md. For the reservoir characterization, other anisotropic values were used. For the final pre-test analysis, the horizontal permeability was defined as 700 md and the net vertical permeability was defined to be 135 md. Analysis of core from the I/W well and the adjacent instrumentation wells provided data that led to the description of vertical permeabilities shown in Figure 3.2. This detail was used in the final pre-test analysis. The data was applied, as shown, only in the vicinity of the I/W well. Grid permeabilities were defined so that the permeability layers remained approximately parallel to the caprock. Beyond a radius of 108 m (which coincides with a computational grid line), the net vertical permeability of 135 md was applied.

The saturation functions have not been defined from Pittsfield core. The functions used were typical of St. Peter sandstone from other areas and were as applied in Wiles (1979a). The equations for the relative permeability to air and water are, respectively,

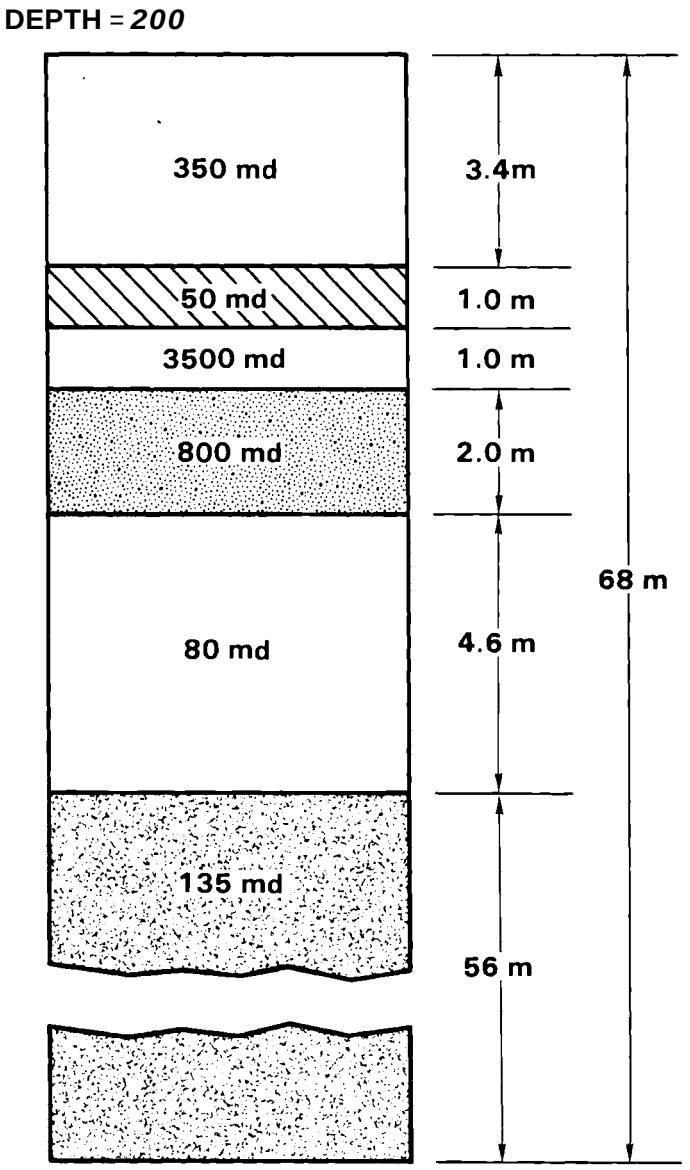

FIGURE 3.2. Stratified Vertical Permeabilities Used in Final Pre-Test Analysis

$$k_{r,air} = (0.90 - S)^2 \, [2.34 - 1.37 \, (0.90 - S)^2] \quad (3.1)$$

$$k_{r,water} = (S - 0.20)^3 \, [4.93 - 3.72 \, (S - 0.20)] \quad (3.2)$$

where S is the saturation, defined here as the fraction of the pore volume containing liquid water.

The capillary pressure function is

$$P_c = \frac{0.05525}{S - 0.15} - 0.065 \text{ atm} \quad (3.3)$$

These functions are shown in Figures 3.3 and 3.4.

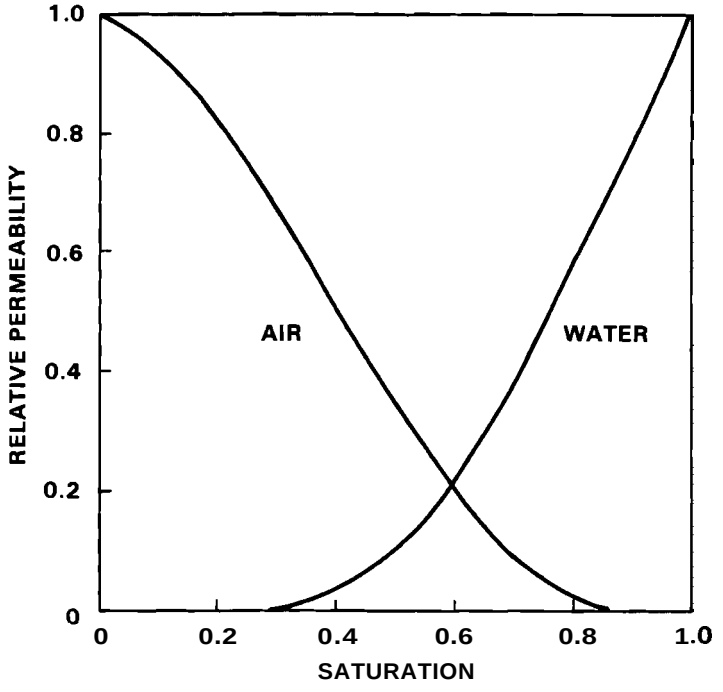

FIGURE 3.3. Relative Permeability Functions

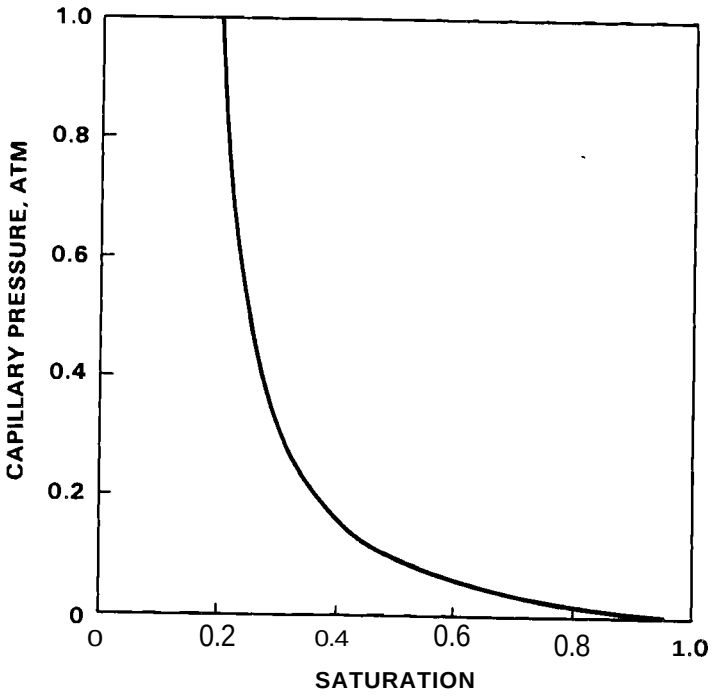

FIGURE 3.4. Capillary Pressure Function

The limits on the saturation functions are important to the outcome of the analysis and should be noted. The relative permeability to air goes to zero for a liquid saturation of 0.9; i.e., for the air to be mobile it must represent at least 10% of the pore volume. This means that if water refloods a region, at least 10% of the pore volume in that region will contain residual or trapped air. However, subsequent pressurization may result in a saturation that is greater than 0.9. The relative permeability for water goes to zero at a liquid saturation of 0.2. Thus, without phase change, this function, Equation (3.2), dictates that 20% of the pore volume will contain liquid water when all of the mobile water has been displaced. This has a significant impact on the extent that water can be displaced from the air storage zone. Finally, at the residual water saturation of 0.2, the capillary pressure is 1 atm. This means that the vertical thickness of the capillary transition zone at equilibrium will be about 10 m, corresponding to the height of a water column that effects a pressure of 1 atm.

Other assumed properties include the porosity (20%), the rock thermal conductivity (2.16 W/m-°C), and the rock thermal capacity (2.62 MJ/m^3-°C).

The operating conditions include a discovery pressure of 145 psia (1000 kPa), a maximum injection pressure of 290 psia (2000 kPa), and a maximum injection flow rate of 1250 scfm (0.723 kg/sec). To initiate bubble development, the bottomhole pressure was ramped linearly from discovery pressure to the maximum pressure over a period of 24 hours. The bottomhole pressure was then held constant throughout the remainder of the bubble development. Air injection was continuous. A number of schedules were used to characterize the reservoir performance during the subsequent air cycling. For all of the air cycling analyses, the air injection rate was a maximum of 1250 scfm. For skewed cycles, lower withdrawal air mass flow rates were used to effect a mass balance in the reservoir. The lower withdrawal mass flow rate results in approximately equivalent volume flow rates for injection and withdrawal at the wellbore/sandface interval. This is a result of the difference in wellbore pressure necessary to effect injection or withdrawal. The final pre-test analysis used a mass balanced cycle that included 7 hr of injection at 1250 scfm, 11 hr of withdrawal at 795 scfm, and 6 hr of closure daily. The reservoir was closed on weekends.

4.0 MODEL DESCRIPTION

The reservoir characterization and pre-test analyses were performed with numerical models developed previously at PNL (Smith, Wiles and Loscutoff 1979; Wiles 1979a, b; Wiles and McCann 1981). The analysis of bubble development and water coning used the two-dimensional, two-phase, isothermal model described in Wiles and McCann (1981). This model includes capillary pressure and relative permeabilities. The thermal analysis was performed with the two-dimensional, single-phase model described in Wiles (1979a). The analysis of the near-wellbore desaturation used the one-dimensional, two-phase model described in Wiles (1979b). This "desaturation model" does not include liquid mobility. It also is based on the assumption that the air-vapor mixture and liquid water are in continuous equilibrium.

These models were written to evaluate specific aspects of reservoir performance and, therefore, can be described as "separate effects" models. These models were particularly useful in evaluations of specific reservoir parameters dealing with geometry, material properties, and operating conditions. They were used to characterize the fundamental performance phenomena of bubble development, water coning, thermal development, and near-wellbore desaturation. The reservoir parameters important to each phenomenon were identified and the effect of variations in each parameter was evaluated on a relative basis. Because the parametric results were compared on a relative basis, it was not crucial that the actual physical coupling of the separate effects was not accounted for by a single model. Even in the field test reservoir characterization analyses, the coupling of physical phenomena in the reservoir was not necessarily required. For example, it was found that the bubble growth rate during bubble development depends on the horizontal permeability and is almost independent of vertical permeability. This conclusion would not likely be affected by a more accurate analysis that included simultaneous thermal development and phase change that may occur during bubble development. Thus, the separate effects models remain as useful, economic tools for reservoir evaluation.

When it comes to actual analysis of reservoir performance, however, the separate effects models may not provide accurate results for all aspects of reservoir behavior. The required accuracy may depend on the strength of the coupling between the various performance phenomena. For example, the saturation distribution near the wellbore will be influenced by desaturation resulting from the injection of slightly heated, very dry air. However, resaturation may occur due to capillary forces. Near-wellbore dehydration will somewhat inhibit thermal growth. The advance and retreat of water may also smear the thermal front by convection and alter the effective thermal conductivity in the air storage zone. As thermal development proceeds, withdrawal air temperatures increase, thereby reducing the air density. To achieve a prescribed air mass flow rate, the velocity must increase. This increases the potential for water coning. All of these effects are coupled to some degree. The performance predictions will eventually be compared against field test data. This comparison should identify the strength of the coupling. The results' may suggest the necessity for a "combined effects" model that couples the two-phase flow equation with an energy equation that includes phase change. At any rate, the results of the pre-test analysis should be viewed with the appropriate limitations in mind.

5.0 RESERVOIR CHARACTERIZATION

The analysis of the Pittsfield reservoir evolved continuously as new data and operational strategies were reviewed. As a result, the initial part of the analysis appeared as being parametric; most of the analysis evaluated reservoir permeability and operational strategy. The results are sufficient to characterize the reservoir performance. There is now a logical basis for explaining reservoir behavior and to resolve discrepancies among field data, laboratory data, and model predictions. This permits quick reevaluation of operational strategy, should unexpected behavior occur in the field. Examples of this would be water production or loss of closure due to fingering.

Each of the four fundamental problems of bubble development, water coning, thermal development, and near-we11bore desaturation were addressed. The emphasis was on the first two problems. Water coning predictions, the outcome of the isothermal air cycling analysis, also provide data on pressure response. The analysis and results of each topic are presented in the following sections.

5.1 BUBBLE DEVELOPMENT

The first bubble development calculation was done with an isotropic, homogeneous permeability of 700 md. The injection/withdrawal zone extended 3.0 m from the top of the reservoir. In this analysis the equivalent mass of water standing in the wellbore was injected into the reservoir prior to the initiation of air injection. The water injection required about 3.5 hr. Air injection was then initiated and continued for 60 days. Following that time, the reservoir was closed in for another 30 days. During the closure period, the reservoir equilibrates toward the hydrostatic pressure and the gravitational and capillary forces. The advance of the 50% saturation front through this period of air injection and reservoir closure is shown in Figure 5.1. The numbers to each curve represent the injection time in days. The 50% saturation front was chosen

to represent the bubble growth because there is very little air ahead of the front and the water ahead of the front is highly mobile. Behind the front, the water mobility is low and the air contained. behind the front represents most of the final equilibrium storage volume of air. Note that the scale of the axis in Figure 5.1 is compressed by about 10 to 1 horizontally. In reality the bubble is extremely flat. Initially, however, the bubble growth is somewhat spherical as there is a strong downward component. After a short time, the downward thrust of the bubble slows dramatically as the bubble pressure, capillary pressure, and gravitational forces approach an equilibrium beneath the well.

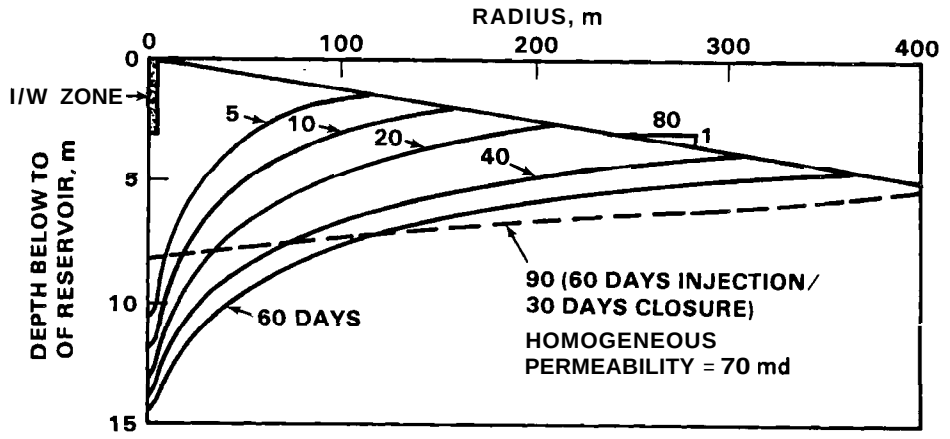

FIGURE 5.1. Bubble Development - Advance of the 50% Saturation Front

The bubble development simulation was intended to answer at least two questions: 1) how long would it take to develop a bubble of adequate size, and 2) would the field test compressor package be adequate? Two measures determine whether the bubble size is adequate. First, there must be enough stored air so that the average pressure in the reservoir is not dramatically affected during the subsequent air cycling. A maximum pressure deviation of about 10% is considered satisfactory. In the field test the injection and withdrawal periods are expected to be less than 1 day. The air flow rates during cycling will be about the same as those during bubble development. Because the computational simulation of bubble

development represented 60 days of continuous air injection, the cycled air mass then represents approximately 1% of the total stored air mass. Therefore, with regard to this criterion, adequate bubble size is achieved. The second measure of adequate bubble size is the vertical distance between the bottom of the wellbore and the air-water interface. This separation is necessary to reduce the potential for water production via water coning. Whether or not water coning will occur during cycling cannot be determined a priori. Water coning is dependent on other, more subtle geologic factors than permeability and operational schedule considered here. The determination of adequate bubble size based on this second criterion is, therefore, subject to some judgment. In our view, the size achieved after 60 days was considered to be adequate. Further analysis with new laboratory or field data may suggest a need to adjust this time.

The injection permit from the Illinois Environmental Protection Agency (IEPA) states that the maximum injection pressure is 300 psig and the maximum injection flow rate is 1250 scfm. The compressor was sized to achieve these limits. In Figure 5.2 the air injection rate is shown for the constant bottomhole pressure of 275 psia used in this analysis. No attempt was made to limit the flow rate as it exceeded 1250 scfm. This would require that the injection pressure drop below 275 psia. However, the discrepancy is small and the general conclusion is that the compressor size is adequate.

A unique feature of the results shown in Figure 5.2 is the drop in flow rate that occurs when the injection pressure reaches its constant value at 24 hours after the start of air injection. The exact cause of this response is not known. One possible explanation is that there are two components of bubble growth: radial and vertical. The vertical growth is a response to the bubble pressure, as well as to gravitational and capillary forces. When the bottomhole pressure ramp ends, the vertical growth slows dramatically. For a relatively high vertical permeability, the vertical growth is a significant part of the total bubble growth. When

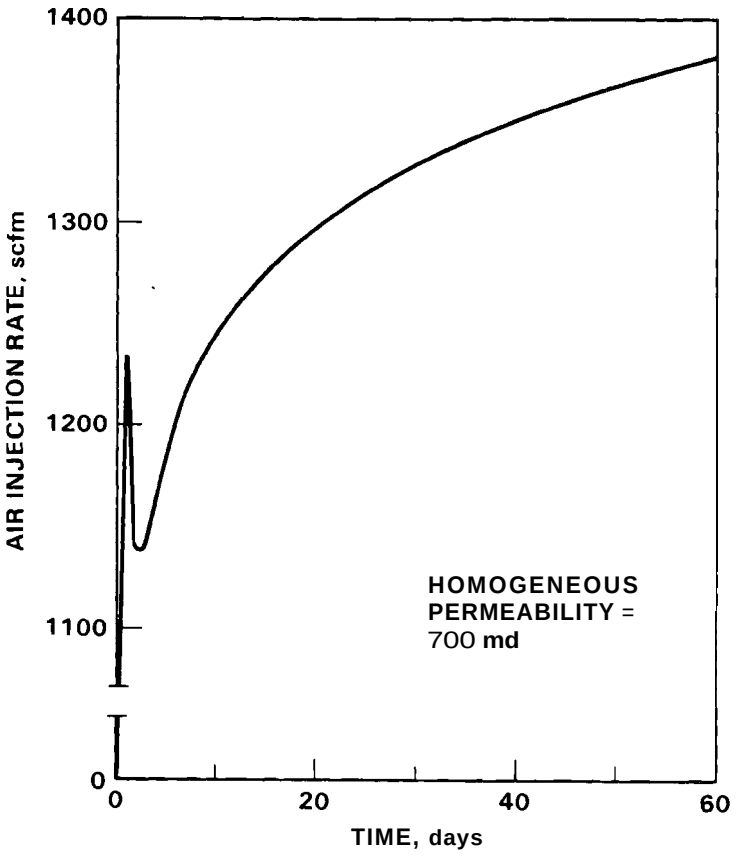

FIGURE 5.2. Air Injection Rate During Bubble Development

the vertical growth slows, it is seen as a noticeable drop in total injection flow rate. This results in the decrease in injection flow rate seen in Figure 5.2.

The growth of the bubble following reservoir closure is due to the existing overpressure. At the initiation of the closure, the average bubble pressure is nearly equal to the injection pressure of 18.7 atm. Meanwhile, the hydrostatic pressure is 10 atm. The bubble continues to expand to approach an equilibrium with the hydrostatic pressure. The decay of the bubble pressure is shown in Figure 5.3 for two locations in the reservoir. Following an initial rapid transient of the injection zone

pressure, the entire bubble responds uniformly to the equilibration process. Gravitational forces cause the constant saturation fronts to approach the horizontal. This is most noticeable in Figure 5.1 where the region below the wellbore is reflooded during reservoir closure. Superimposed on these two primary equilibration mechanisms is the effect of capillary forces. These drive the vertical saturation distribution more slowly to a capillary-gravitational equilibrium.

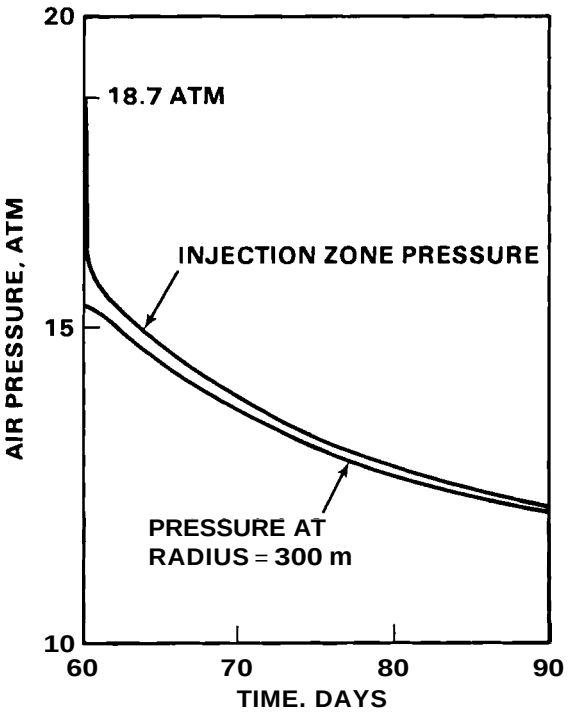

FIGURE 5.3. Pressure Equilibration During Reservoir Closure

Other values of permeability were examined in simulations of bubble development. In Figure 5.4 the advance of the 50% saturation front is shown for a horizontal permeability of 3500 md. The vertical permeability was 700 md. Comparable times in the simulation were superimposed from Figure 5.1. The results of this analysis showed the' significant influence of the horizontal permeability on the bubble development. An initial analysis with the high value of horizontal permeability used a bottomhole pressure of 275 psia after the startup pressure ramp. For this case the

reservoir was taking air at approximately 5900 scfm, far in excess of compressor capacity and the IEPA limit. The simulation was repeated with the injection flow rate limited to 1250 scfm. This is the case shown in Figure 5.4. For this case the bottomhole pressure was initially about 200 psia. As the bubble development progressed, the required bottomhole pressure dropped gradually and was about 185 psia at the conclusion of the simulation. With the large value of horizontal permeability, the reservoir would take air with relative ease.

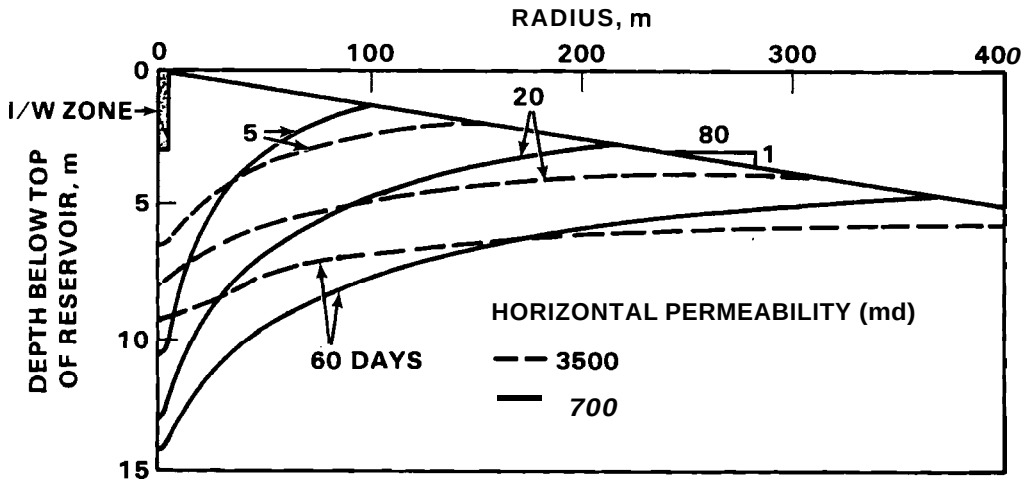

FIGURE 5.4. Bubble Development - Advance of the 50% Saturation Front with Different Horizontal Permeabilities

In Figure 5.5 the advance of the 50% saturation front is shown for a vertical permeability of 350 md. The horizontal permeability was 700 md. Selected results from Figure 5.1 were superimposed for comparison. The air injection rates are compared in Figure 5.6. The curve for 700 md repeats Figure 5.2. These results indicate that the vertical permeability has only a small effect on bubble development. In Figure 5.6 the decrease in air injection rate, discussed in reference to Figure 5.2, occurs for the low permeability case as well. The fact that the magnitude of the decrease is not as great for the low permeability case led to speculation on the cause

of the behavior. With a lower vertical permeability, the downward growth of the bubble represents a smaller component of the total air injection. When this component is reduced as the bottomhole pressure reaches a constant value, there is less effect on the total flow.

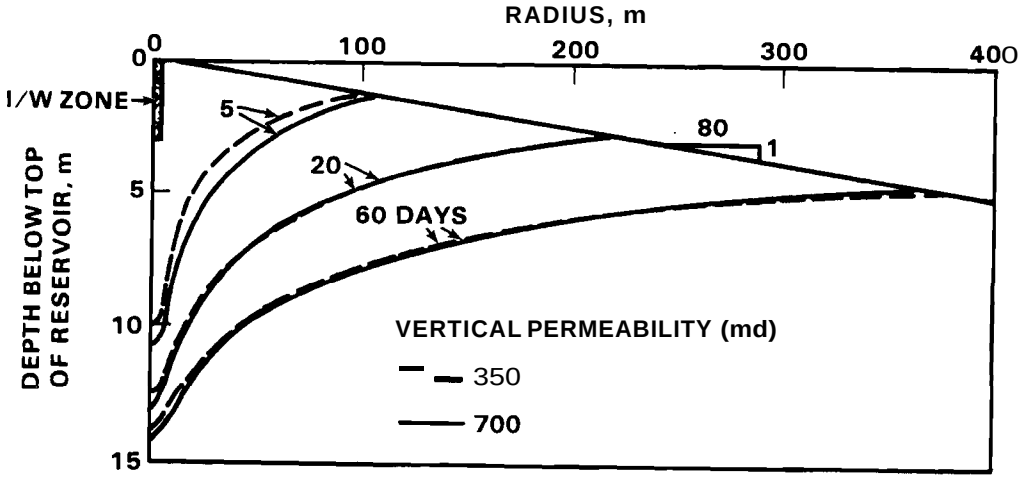

FIGURE 5.5. Bubble Development - Advance of the 50% Saturation Front with Different Vertical Permeabilities

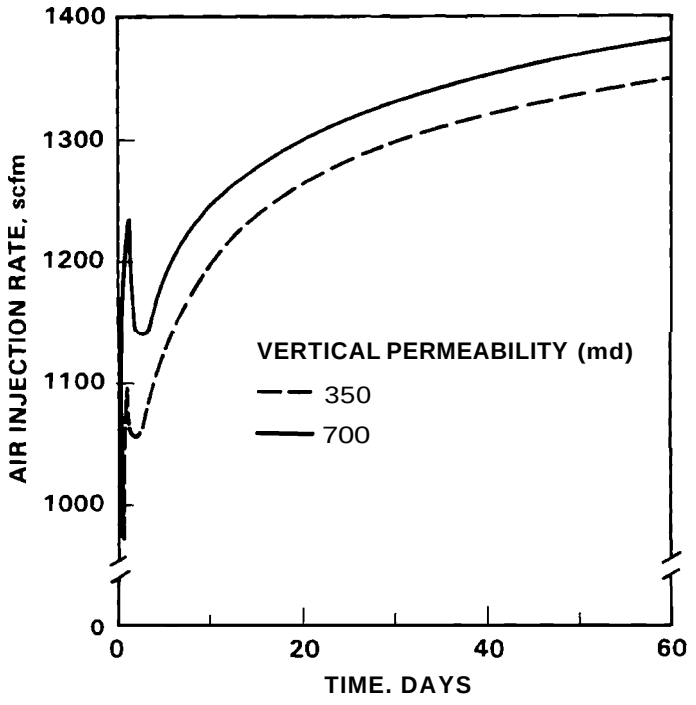

FIGURE 5.6. Air Injection Rate During Bubble Development 'With Different Vertical Permeabilities

Another parameter investigated with regard to bubble development was the elevation of the injection/withdrawal zone relative to the top of the reservoir. This analysis was performed because the casing for the I/W well extended well below the bottom of the caprock. The I/W zone was defined to extend from 2.4 to 5.0 m below the bottom of the caprock for this analysis. When the air was injected at this elevation in the bubble development simulation, the extremely buoyant air merely rose to the top of the reservoir where the displacement of water was initiated. The result was that the saturation distribution at the completion of bubble development was, for all practical purposes, totally independent of this change in injection elevation. Thus, for the lower injection elevation the air-water interface was much closer to the I/W zone at the conclusion of bubble development. During the subsequent analysis of air cycling, the wellbore flooded before the end of the initial air withdrawal cycle. This terminated the simulation. The impact of this calculation on the field test was that the casing was perforated at the top of the formation rather than setting a gravel pack and screen below the completed casing.

5.2 ISOTHERMAL AIR CYCLING

The primary purpose of the isothermal air cycling calculations was to define the potential for water production to occur during the field test. The results also provided the bottomhole pressures that were required to achieve the prescribed air mass flow rates.

Water coning is depicted in Figure 5.7. During air withdrawal, pressure gradients cause air to flow toward the wellbore. Mobile water that exists within these pressure gradients will also flow toward the wellbore. The velocities of the air and water are determined by the local pressure gradient and their respective mobilities. As the mobile water exists closer to the production interval of the wellbore, there will be a greater potential for water to rise toward the wellbore. This increase of water saturation below the wellbore is called water coning. During air cycling, water will rise toward the wellbore when air is withdrawn. Water

will recede during air injection. Eventual water production depends on the combined net effect of the relative length of the injection and withdrawal cycles, the pressure gradients and the fluid mobilities; these topics are discussed in the following paragraphs.

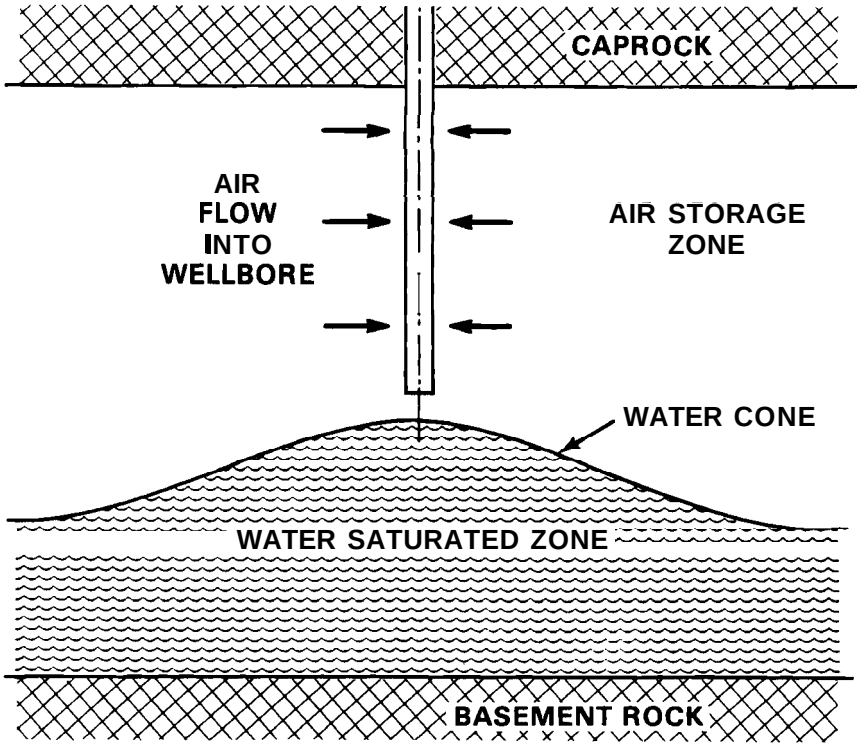

FIGURE 5.7. Water Coning

A parametric evaluation of water coning for conditions typical of a commercial CAES facility was reported in Wiles and McCann (1981). Conditions at the Pittsfield site that increase the potential for water production to occur relative to a commercial facility are that the air storage zone is vertically thin and is at low pressure. Because the air storage zone is vertically thin, mobile water will be present throughout the air storage zone at the conclusion of bubble development. This mobile water, retained in the bubble by capillary forces, could be produced as air cycling begins. The amount of water production from this source could be

significantly reduced if near-wellbore desaturation due to the injection of undersaturated air dries this region during bubble development. Heterogeneous bedding features, such as thin shale beddings not obvious in core sections, can also alter actual response.

Because the field test air storage zone is at relatively low pressure, there are significant differences in the bottomhole air densities between the injection and withdrawal sides of the cycle. If the air mass flow rates on both sides of the cycle are equal, then the sandface air velocity would be greater during the withdrawal phase. This would require that the pressure drop across the reservoir be greater during withdrawal. Because this cycle would have equal injection and withdrawal times to maintain a constant air mass in the reservoir, there would be a net pressure gradient driving water toward the wellbore. This source of water coning can be controlled to some extent by implementing a skewed cycle, i.e., by withdrawing air at a reduced mass flow rate over a longer period of time, relative to the injection cycle. By this mechanism the pressure drop across the reservoir can be approximately balanced on both sides of the cycle. The actual volume flow rate, as measured at the sandface, would also be nearly equal.

The mobility of the water plays a role equal to the importance of the pressure gradient in determining the potential for water coning. When water rises toward the wellbore, the water cone is fed from below where the saturation is comparatively high. Here, the relative permeability to water, which effectively defines the liquid mobility, is also high. When the water cone recedes during air injection, water must drain out of regions where the saturations and, therefore, the relative permeability to water, are decreasing. The result is that there can be a significant imbalance in mobilities on opposite sides of the injection/withdrawal cycle. Unlike the pressure gradients, essentially nothing can be done to control these mobilities. Only a low net vertical permeability in the vicinity of the wellbore can reduce the liquid mobility sufficiently to preclude or inhibit vertical water migration.

The key elements of water coning are vertical permeability and the operational scheduling. These parameters were investigated in the analysis of isothermal air cycling.

5.2.1 Vertical Permeability Effects on Water Coning

The simulation of isothermal air cycling to define the potential for water coning was initiated from a solution for bubble development. At the conclusion of bubble development, the average bubble pressure was significantly greater than the original hydrostatic pressure. Thus, the bubble continued to expand when the injection air flow was terminated. This expansion allowed the bubble to approach an equilibrium with the hydrostatic background pressure. Also, the region below the wellbore, where the air-water interface was depressed, reflooded as the saturation distribution flattened to approach a capillary-gravitational equilibrium. This is shown in Figure 5.1 by the 90-day profile, a solution defined by 30 days of reservoir closure. In the analysis of water coning, these two factors, bubble expansion and capillary-gravitational equilibration, resulted in a redistribution of the saturation due to the pressure gradients existing during air cycling. It was not practical to separate these effects because the important issue was to define the conditions under which the saturations increased. This would define the potential for water production to occur in the near-wellbore vicinity during air cycling.

The nominal value of permeability was defined to be 700 md. The only other value used in this general reservoir characterization analysis of water coning was a vertical permeability of 350 md. The air cycling calculations require a bubble development solution for each value of permeability. The vertical saturation distribution at the center of the reservoir, a region which includes the injection/withdrawal well, is shown in Figure 5.8 for the beginning of air cycling and after 2 weeks of air cycling. For this case the air cycling begins after 30 days of reservoir closure that followed 60 days of continuous air injection to develop the air storage bubble. The cycle defined for this calculation was 12 hr of air withdrawal and 12 hr of air injection. The air mass flow rates were

1250 scfm on both sides of the cycle. This cycle was repeated without closure or other interruption. As expected, the results show that the saturation buildup is more severe for the case of higher vertical permeability. However, there is significant water buildup for both cases of vertical permeability. These results suggest that the vertical permeability will have to be much lower to preclude eventual water production with this cycle.

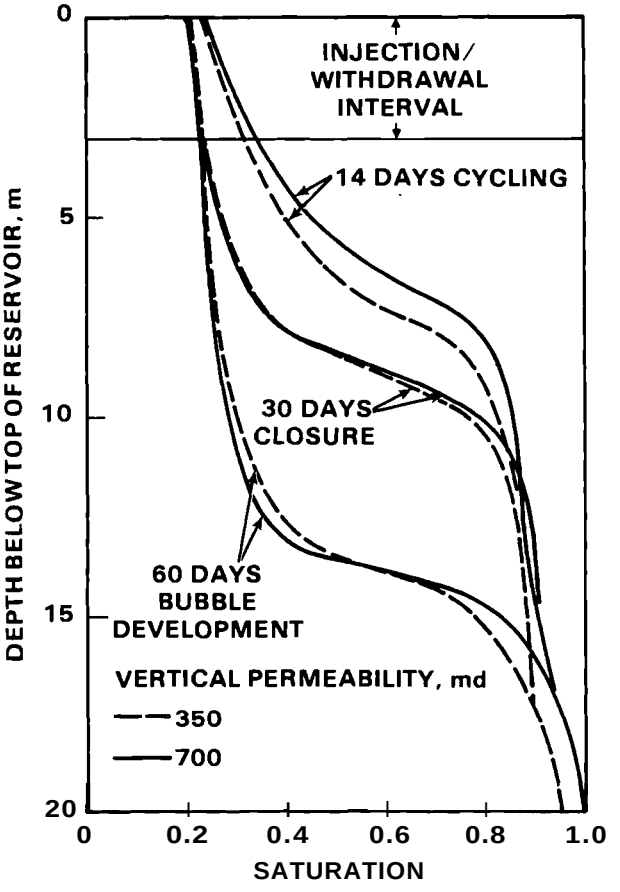

FIGURE 5.8. Vertical Profiles of Saturation at the Center of the Reservoir with Different Vertical Permeabilities

The results of the simulations also suggest the relative importance of the redistribution of fluids as the air storage bubble responds to the ambient conditions. Much of the increase in saturations shown in

Figure 5.8 occurs in the 30 days of closure following bubble development. The region below the injection/withdrawal zone is reflooded as capillary-gravitational equilibrium is approached.

The process by which the saturation increases at a given location is demonstrated in Figure 5.9, where the increase in saturation for the two assigned values of vertical permeability are also compared. The location is 5.75 m below the caprock and 2.75 m below the bottom of the injection/withdrawal interval. This location was chosen to demonstrate the behavior because the saturation changes are most pronounced. In general, the behavior is similar at other locations although the amplitude of the cyclic saturation changes is reduced. The saturation increases during air withdrawal and decreases during the subsequent air injection. The net effect is a cycling of the saturation between two bands. A gradual increase in saturation with time is noted; the amplitude of the saturation cycles is approximately proportional to the vertical permeability and the rate of net saturation change is only slightly different for the two cases. After a period of time that would be relatively short compared to the duration of the field test, the average saturation at a location would be expected to be independent of vertical permeability. This results because, as the saturation increases, the relative permeability of the air decreases, thereby reducing the mobility of the air. Air must be displaced for the saturation to increase. For the higher vertical permeability, the relatively rapid increase in saturation at the outset of air cycling causes the mobility of the air to be reduced to a value comparable to that for the lower permeability case. Beyond that initial transient, the displacement of air and the increasing saturation occur at nearly equal rates for both values of absolute vertical permeability.

5.2.2 Operational Control of Water Coning

Three operational strategies were evaluated to determine their potential effectiveness on the control of water coning. Each of these strategies is limited by the time and resources available for the field

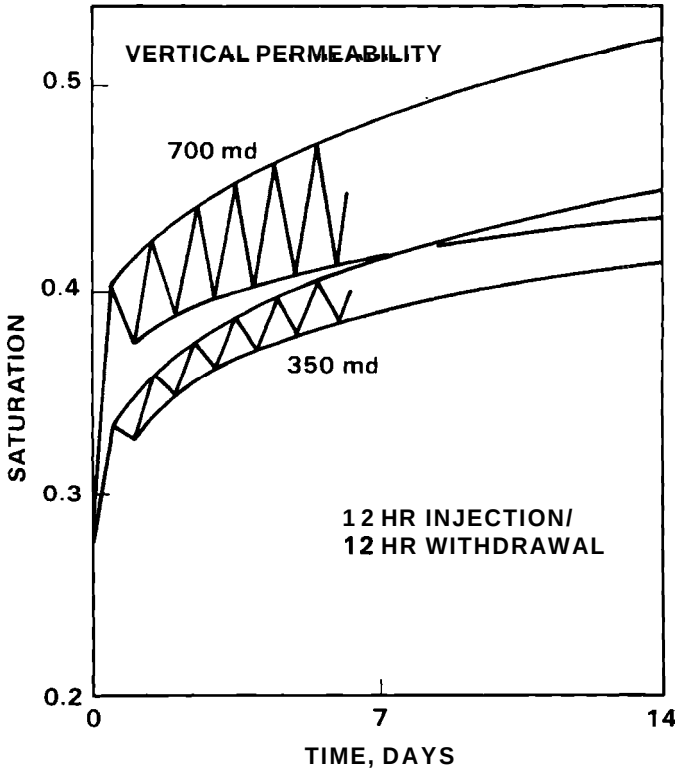

FIGURE 5.9. Saturation Histories 5.75 m Below the Caprock at the Center of the Reservoir with Different Vertical Permeabilities

test, as well as by the impact that these strategies might have on other aspects of the field test. These strategies included additional bubble development, cycle duration, and skewed cycles. A fourth strategy is to reduce the maximum flow rates. This was not pursued because such an approach might have an unacceptable impact on other aspects of the field test; e.g., it would reduce the total thermal energy that could be injected in the reservoir.

Additional bubble development was evaluated with the idea that the air-water interface could be further depressed vertically, thereby increasing the separation of the interface from the injection/withdrawal interval. The location of the 50% saturation front is shown in Figure 5.10. Thirty days of additional air injection results in an additional 1-m depression of the air-water interface. This would certainly

delay water production but would not preclude its occurrence. In consideration of the constraints on time and resources for the field test, the benefit of additional air injection was not pursued further.

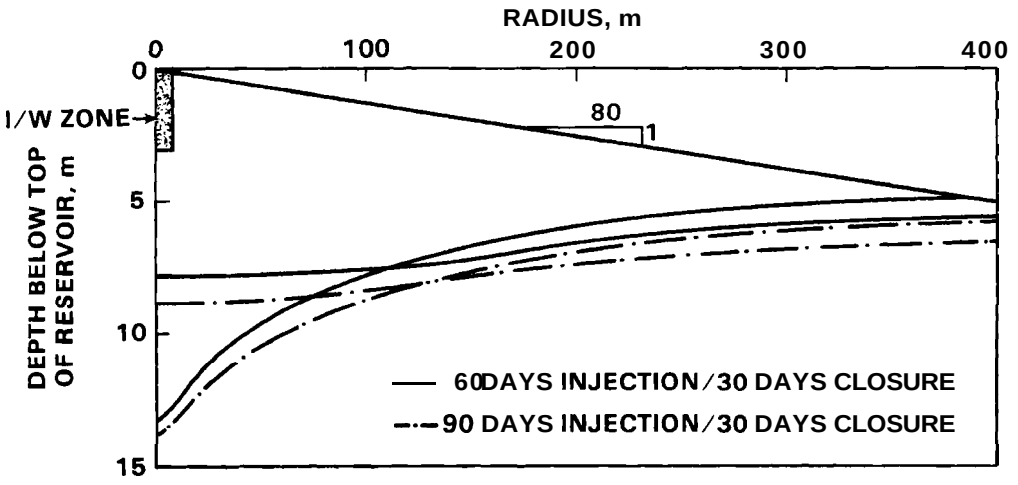

FIGURE 5.10. Additional Bubble Development to Avoid Water Coning

The cycle duration refers to the time span of the injection/withdrawal and any closure that may occur as part of the complete cycle. Two cycles were compared to the 12-hr withdrawal/12-hr injection cycle indicated in Figure 5.9. Other cycles evaluated were 12-hr withdrawal/12-hr injection with weekend closure, and 6-hr withdrawal/6-hr injection. A vertical permeability of 350 md was used in this evaluation of cycle duration.

It was observed that the 12-hr withdrawal/12-hr injection cycle resulted in a net increase in saturation in the vicinity of the wellbore. Adjusting the cycle to include weekend closure was proposed to allow time for gravity drainage to return the saturations to the same values at the beginning of each week. Adjusting the cycle to include shorter withdrawal and injection periods was proposed because it was believed that this action would reduce the rate of water advancement toward the wellbore.

The saturation at a given location changes according to the description presented for Figure 5.9. The saturation changes for the two other cycles are shown in Figures 5.11 and 5.12. In each case the location is 5.75 m below the caprock at the center of the reservoir. The three cycles are compared in Figure 5.13. The weekend closure does result in some decay of the saturation and increased mobility of air. During the initial withdrawal after the weekend closure, the air is readily displaced and the saturation rebounds almost as if the closure had never occurred. The 6-hr cycle results in a reduced amplitude of saturation cycling but the rate of net saturation change is almost independent of the length of the cycle. This behavior is also explained by consideration of the changes in mobilities. The longer cycle results in a greater increase in saturation during the first withdrawal. This leaves the water more mobile. Coupled with the longer injection time, the increased mobility allows the saturation to decay further during the injection cycle.

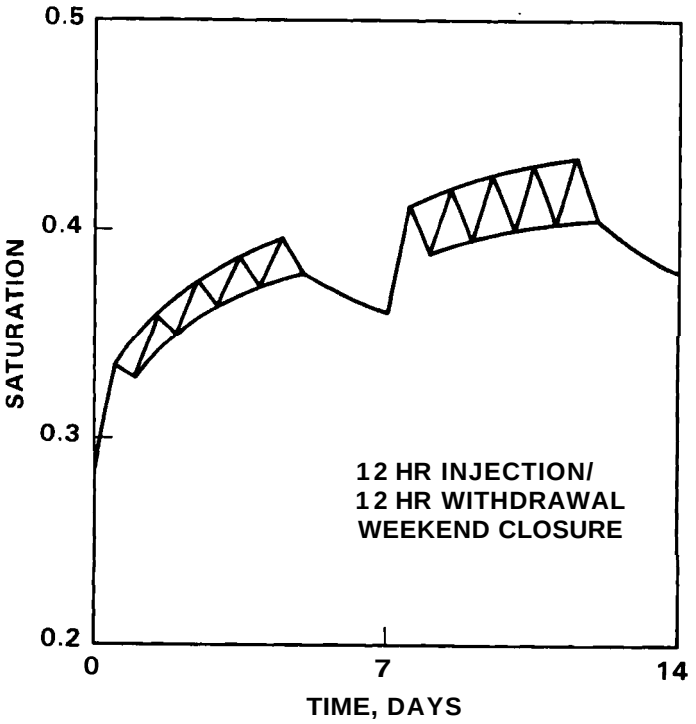

FIGURE 5.11. Saturation History for 12-hr Injection/12-hr Withdrawal, with Weekend Closure

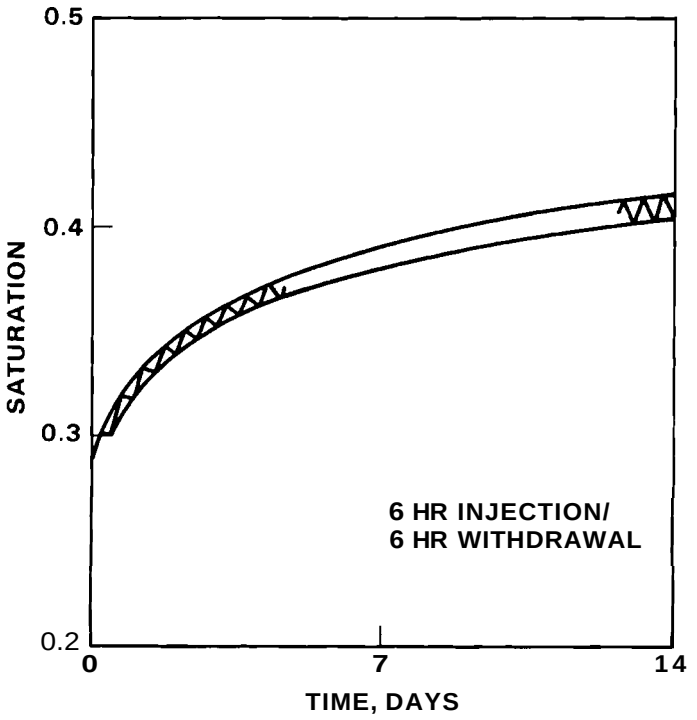

FIGURE 5.12. Saturation History for 6-hr Injection/6-hr Withdrawal

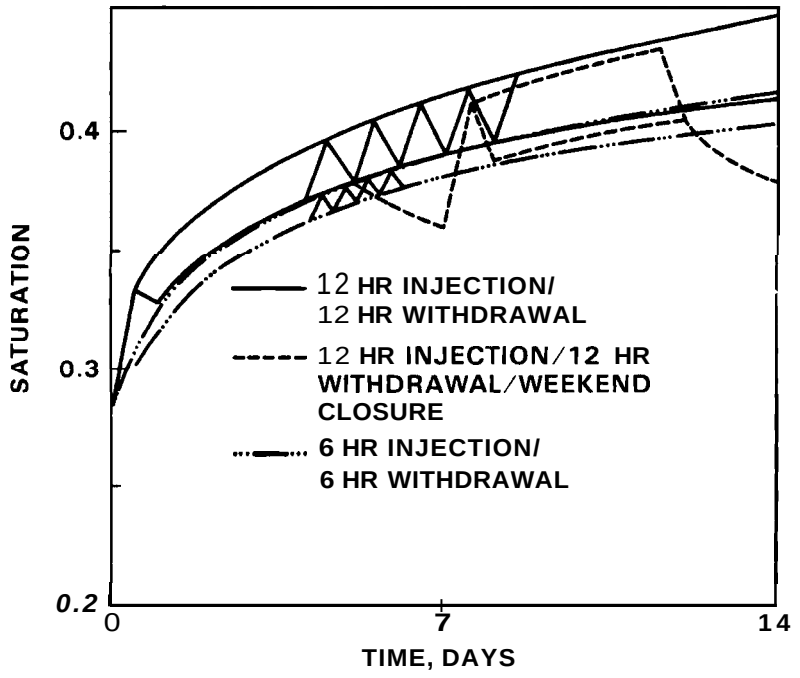

FIGURE 5.13. Comparison of Saturation Histories for Cycles of Various Duration

From this analysis it is concluded that adjustment of the cycle duration parameters will not significantly affect the potential for water coning.

A skewed injection/withdrawal cycle refers to a cycle having unequal injection and withdrawal times but an approximate daily mass balance. To reduce the potential for water coning, the withdrawal time is greater than the injection time. To obtain a net mass balance, the withdrawal flow rates are less than the injection flow rates. Therefore, the pressure gradient is reduced on the withdrawal side of the cycle, reducing the potential for water coning.

The field test site is unique, relative to anticipated commercial conditions, because of the low reservoir pressure. To achieve reasonable flow rates the ratio of bottomhole pressure between the injection and withdrawal cycles can easily be 2 to 1. This creates large density differences. For equal air mass flow rates there would be large differences in air velocity. This would result in large differences in the pressure gradient across the reservoir between the injection and withdrawal cycles. The imbalance in pressure gradients results in a significant net potential for water coning to occur. The skewed cycle can reduce this potential by approaching an approximate balance in the pressure gradients. To achieve a time-integrated pressure balance, the cycle would have to be skewed enough that the reservoir pressure drop during withdrawal is lower than that during injection. In this way the product of the pressure drop and the length of the cycle would be nearly equal for both sides of the cycle.

The skewed cycles that were evaluated included 8 hr of injection/16 hr of withdrawal and 4 hr of injection/20 hr of withdrawal. The 8/16 cycle is approximately pressure-balanced; that is, the pressure gradient between the wellbore and the bulk of the reservoir is approximately the same magnitude

on either side of the cycle. The 4/20 cycle overcompensates the pressure gradient, making the pressure gradient considerably greater on the injection side of the cycle than on the withdrawal side. If pressure gradients due to injection/withdrawal flow rates were the only factor affecting water migration near the wellbore, then the 20/4 cycle would result in a net migration of water away from the well bore.

The saturation histories at a location 3.75 m below the caprock at the center of the reservoir for the two skewed cycles are shown in Figure 5.14 and compared with the 12/12 cycle. On the injection side of each cycle, the air flow rate is 1250 scfm. The withdrawal flow rate is adjusted to achieve a net mass balance in the reservoir. For example; the withdrawal flow rate is 625 scfm for 16 hr for the 8/16 cycle. The permeability applied in the analysis was a homogeneous 700 md. The results show that skewed cycles can significantly reduce the potential for water coning, although for the 4/20 cycle there is still some saturation increase. However, this is most likely due to the continuing equilibration of the bubble rather than imbalanced pressure/mobility driven water coning. The 8/16 cycle shows a moderate increase in saturation during the 2 weeks of simulated air cycling.

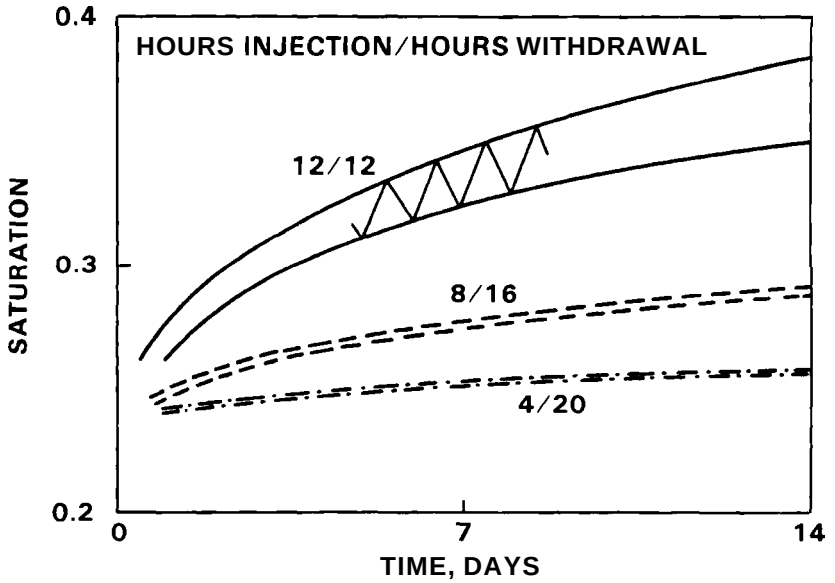

FIGURE 5.14. Comparison of Saturation Histories for Various Skewed Cycles

5.3 THERMAL DEVELOPMENT

The general behavior of thermal development in a CAES reservoir was reported by Wiles (1979a).

Drilling technology limits the distance from the injection/withdrawal well to the surrounding observation wells. For the field test the observation wells were located approximately 2 and 8 m from the injection/withdrawal well. The thermal development calculations were intended to indicate whether or not a heated region could be established beyond this radius within the time frame of the field test, thereby supplying useful thermal development data.

A cycle of 4 hr of injection and 4 hr of withdrawal was selected for this analysis. This was judged to be the shortest conceivable injection period. An injection temperature of 200°C was defined to exist at the bottomhole. Four weeks of cycling were simulated. Radial temperature profiles are shown in Figure 5.15. These profiles were taken along the top of the reservoir at the conclusion of the final withdrawal cycle for each week. If thermal recovery from the reservoir were complete, no thermal buildup would occur. Therefore, these curves represent the nonrecoverable thermal energy lost to the reservoir. Because peak recovery temperatures increased, then the rate of thermal loss to the reservoir decreased, as one might expect. The temperature dip near the well bore was due to the effects of cooler air being drawn from below.

The results of the preliminary thermal development analysis suggest that some thermal data should be obtainable at the observation wells. Results for longer cycle durations were even slightly more favorable in this regard. A longer injection cycle carries heated air farther into the reservoir where it dissipates more readily. For a cycle of 12 hr injection/12 hr extraction, the peak extraction temperature after 4 weeks is about 131°C which compares to a value of about 145°C for the 4-hr injection/4-hr extraction cycle shown in Figure 5.15. The longer cycle duration will not only promote greater thermal development but will also result in more temperature cycling at the observation wells.

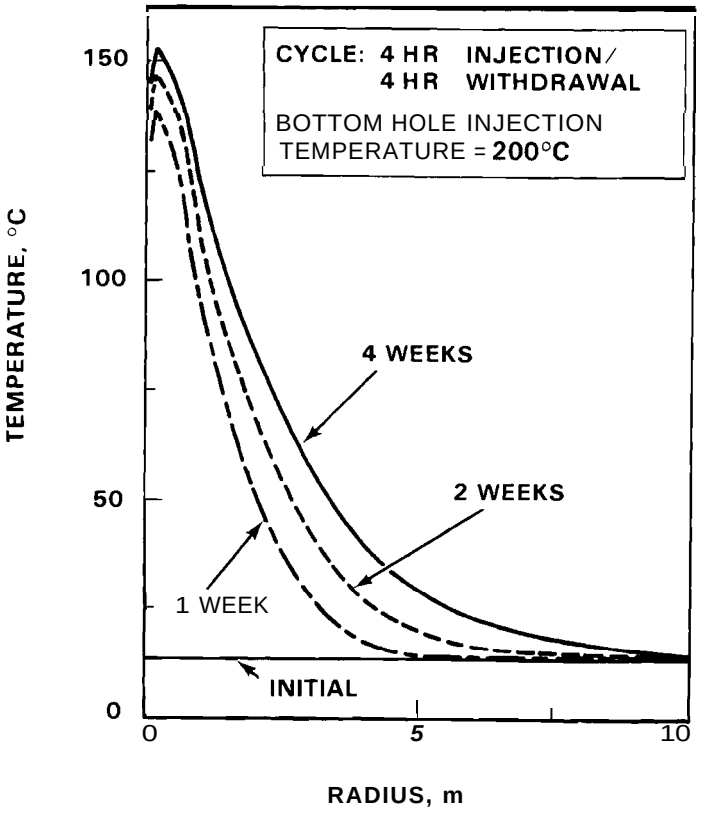

FIGURE 5.15. Thermal Development - Radial Profiles of Temperature After Final Weekly Withdrawal Cycles

In spite of these positive indications of thermal performance, the following factors could contribute to a less favorable result:

- Heat losses between the above-ground equipment and the reservoir have not been accounted for.
- Dehydration in the near-wellbore region will inhibit thermal growth.
- The advance and retreat of underlying water will smear the thermal front.
- To avoid water coning, long withdrawal cycles at low flow rates may be necessary. In the time frame of the field tests, this would reduce the total thermal energy to which the reservoir is subjected.

5.4 NEAR-WELLBORE DEHYDRATION

The general behavior of near-wellbore dehydration in a CAES reservoir was examined in Wiles (1979b). It is important to dehydrate the near-wellbore region for two reasons. First, the presence of liquid water reduces the permeability to the flow of air. Second, liquid water in the presence of air and slightly elevated temperatures may cause geochemical reactions that reduce permeability. Reduced permeability in the near-wellbore region implies that a greater pressure gradient is required to achieve a given air flow rate. This would lower the efficiency of reservoir performance and would promote water coning, which would compound the problem.

The dehydration of the near-wellbore region proceeds as follows. During injection of undersaturated air at elevated temperature, the air gains moisture as it moves radially outward. The air temperature also drops as the thermal energy is exchanged with the surrounding media. The air finally reaches a radial position where it is saturated at the local pressure and temperature. As the air moves beyond this point, condensation occurs because the temperature continues to decrease. By this mechanism a dehydrated zone is established around the wellbore. Beyond this so-called "dry front" is a transition region characterized by some saturation buildup.

During the withdrawal side of the cycle, water is also removed from the reservoir. Air moving toward the wellbore gains moisture as it enters the region of increasing temperature. However, it gains moisture only until it reaches the dry front. The air is then withdrawn from the reservoir at a saturated state determined by the pressure and temperature at the location of the dry front.

The analysis of dehydration for the field site reservoir was also based on a cycle of 4 hr of injection and 4 hr of withdrawal. Radial saturation profiles for different times during development are shown in Figure 5.16. These results can be compared against data from the field

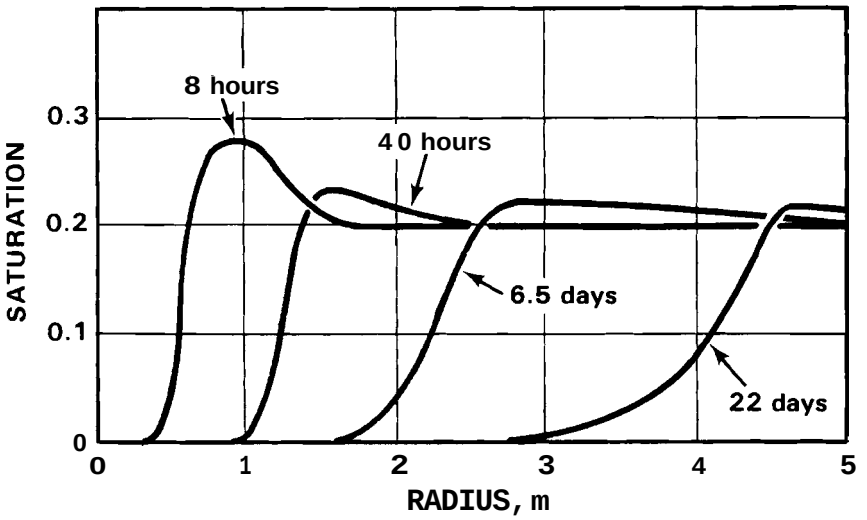

FIGURE 5.16. Dehydration - Radial Profile of Saturation

test where extraction humidity will be monitored. Such a comparison will likely show differences in predicted and actual data for the following reasons:

- If the injection air is undersaturated during bubble development, then a dehydrated zone may already be established around the wellbore when cyclic operation begins. Analysis indicated the dry front may extend as far as 5 m into the reservoir at the completion of bubble development.
- As a dehydrated zone begins to establish, capillary forces in the thin bubble may act to continuously introduce water into the drying region, thereby preventing complete dehydration.
- Water coning may introduce mobile water to the heated zone around the wellbore, thereby increasing outlet humidities.
- An injection humidity of zero, as used in this analysis, is not exactly achievable, although the field test driers come very close. The actual nonzero value reduces the dehydration rate slightly.
- The model assumes that, in the presence of liquid water, the air will be saturated at the local thermodynamic conditions. A proper accounting of this rate process could probably affect the predicted outlet humidity.

6.0 FINAL PRE-TEST ANALYSIS

Prior to the initiation of bubble development operation at the field test reservoir, a final pre-test simulation was run based on our most current knowledge of reservoir properties. The major difference in this simulation involved the refinement of reservoir vertical permeability. The horizontal permeability was defined to be homogeneous at 700 md. Experimental data from PNL and David K. Davies (PB-KBB, Inc., and David K. Davies and Associates 1983) pointed to a wide variation in vertical permeabilities near the top of the St. Peter as measured in core samples from the injection/withdrawal well and the adjacent instrumentation and logging wells. This data was summarized as the stratified permeabilities shown in Figure 3.2. These vertical permeabilities were defined to a radius of 108 m. The grid permeabilities were defined so that a given layer was approximately parallel to the sloped caprock. A reservoir average vertical permeability of 135 md was maintained throughout the remainder of the computational grid. The other conditions of the analysis are given in Table 3.1.

Another important point is that no skin loss (the effect of flow restriction due to the completion method) was defined at the wellbore. This condition is consistent with all previous simulations. The original plan for completion of the injection/withdrawal well called for a gravel pack and screened liner. Such a completion would have added insignificant flow resistance at the wellbore based on previous PNL studies and industry experience. The actual completion involved explosive perforations of the casing. While the resultant completion may have increased the flow resistance at the wellbore, a skin effect was not quantified and, therefore, was not included in this analysis. A significant skin effect could dramatically alter the apparent performance of the reservoir.

Final pre-test simulations were performed only for the two-phase flow problems; i.e., bubble development and isothermal air cycling. This stage of operations was scheduled to take up to 6 months of test operations. The

field data from these operations could then be used for later fluid/thermal analyses prior to thermal development.

6.1 BUBBLE DEVELOPMENT

The bubble development simulation involved 60 days of continuous air injection, followed by 15 days of reservoir closure. The bottomhole pressure is ramped linearly during the first 24 hr of the simulation from a discovery pressure of 145 psia to a maximum pressure of 290 psia. Throughout the remainder of bubble development, air injection the bottomhole pressure remains at 290 psia.

The air injection mass flow rate is shown in Figure 6.1. There is only a slight perturbation of the injection flow rate after the bottomhole pressure stabilizes after 24 hr of injection. When the bottomhole pressure stabilizes, vertical growth of the bubble slows as gravitational and capillary forces quickly equilibrate with the imposed bubble pressure. In this case, with a low vertical permeability the vertical component of bubble growth is relatively small. When the vertical growth slows at the conclusion of the bottomhole pressure ramp, the effect on the total bubble growth rate is minor.

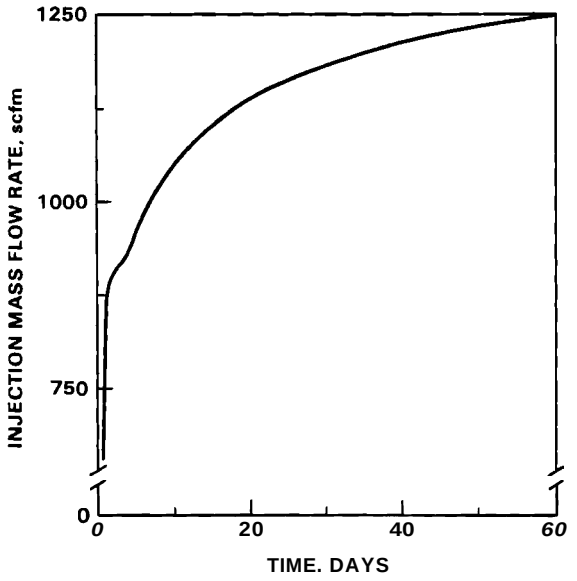

FIGURE 6.1. Air Injection Rate for Bubble Development - Final Pre-Test Analysis

The advance of the 50% saturation front is shown in Figure 6.2. In the early phase of bubble development, fingering of air into the high permeability layer below the wellbore is observed. The fingering gradually disappears because of gravity drainage of water from the more highly saturated overlying regions. The final bubble shape is quite similar to the results shown previously. This supports the conclusion that the vertical permeability is less important than the horizontal permeability in determining bubble development.

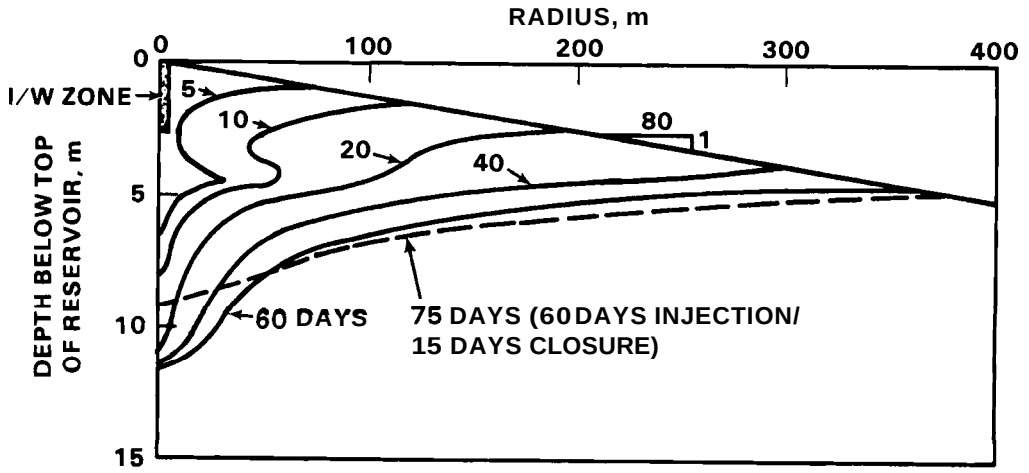

FIGURE 6.2. Bubble Development - Advance of the 50% Saturation Front - Final Pre-Test Analysis

6.2 ISOTHERMAL AIR CYCLING

The goal of this analysis was to define an injection/withdrawal cycle that minimized the migration of water toward the wellbore. Air cycling simulations were initiated from the pressure and saturation distributions defined at the conclusion of the reservoir closure period that followed bubble development.

A number of cycles were tested. The selected cycle was chosen on the basis that the magnitude of the pressure drop between the bottomhole and the bulk reservoir was approximately equal for both the injection and

withdrawal cycle. A time-integrated pressure balance in which the product of the pressure drop and the length of the cycle were equal on both sides of the cycle was not pursued. To achieve that more desirable balance would have required the cycle to be skewed to an extent that other aspects of the field test would be adversely affected. It is only necessary that water production be avoided. If the cycle is skewed enough to accomplish that goal then the cycle is satisfactory.

The cycle that was decided upon as a reasonable balance of the above concerns is 7 hr of injection at 1250 scfm, 11 hr of withdrawal at 795 scfm, and 6 hr of closure. This mass-balanced 24-hr cycle is repeated 5 days a week. On the weekend the reservoir is closed. Ten weeks of air cycling were simulated using this cycle. The 10 weeks is the anticipated length of isothermal air cycling in the field test. After that initial period the injection temperature will be stepped up. This cycle not only achieves an approximate pressure balance, but also approximates the demand curve expected for a typical CAES facility. Also, the air volume flow rates are typical, on the basis of air flow per unit length of the perforated wellbore. This is the measure of similitude between this field test and a full-scale facility.

Several illustrations demonstrate the tendency of water to migrate toward the wellbore. Figure 6.3 shows vertical saturation profiles immediately below the wellbore at the center of the reservoir. The results indicate that, for a reservoir described by the defined conditions and being operated accordingly, water production would not likely be a severe problem. Considerable saturation increases occur in the range of 5 to 10 m below the top of the reservoir. Saturation increases in the immediate vicinity of the wellbore are quite small. This is a result of the low permeability layer below the injection/withdrawal zone. The pressure balance from the skewed cycle also contributes to this favorable result.

Figure 6.4 indicates the movement of the 50% saturation front beginning from the static near equilibrium point after 30 days of closure

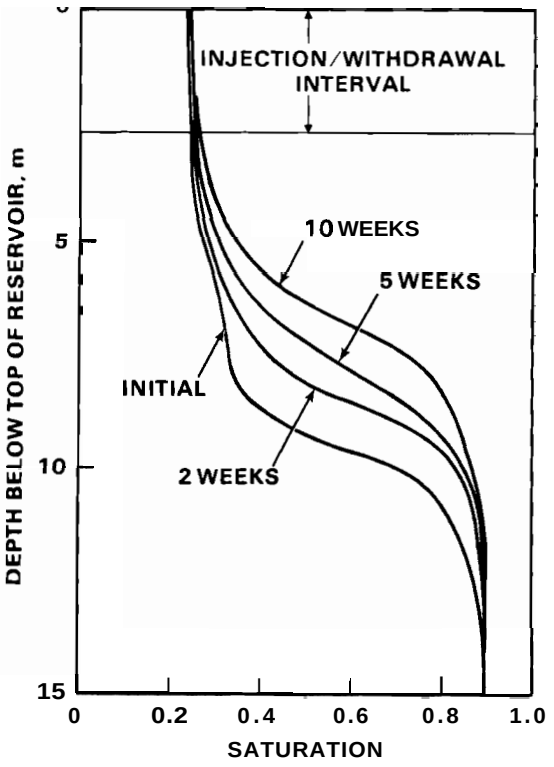

FIGURE **6.3.** Vertical Profiles of Saturation at the Center of the Reservoir - Final Pre-Test Analysis

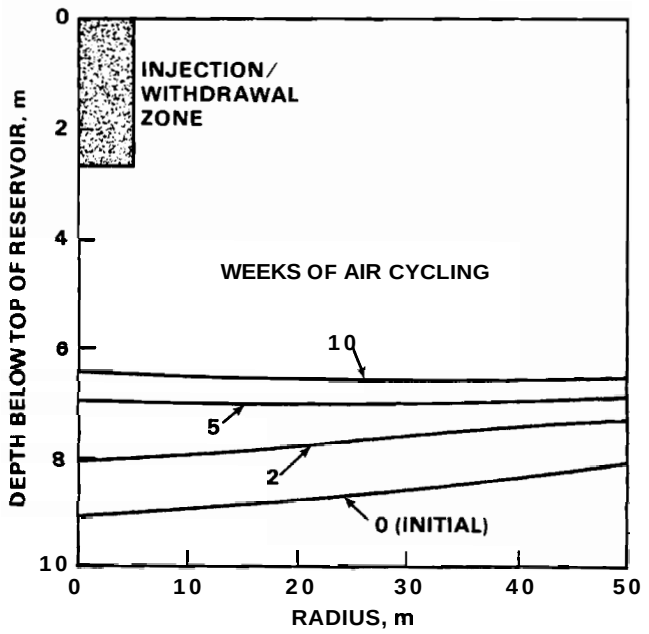

FIGURE 6.4. Advance of the 50% Saturation Front - Final Pre-Test Analysis

following bubble development. As time advances, the saturation profiles approach being horizontal. This suggests that much of the saturation increases below the wellbore are due to continued equilibration of the air storage bubble rather than being the result of water migration driven by pressure and mobility imbalances. During this fairly long-term equilibration period, the region below the wellbore continues to reflood. This process is demonstrated in Figure 6.5.

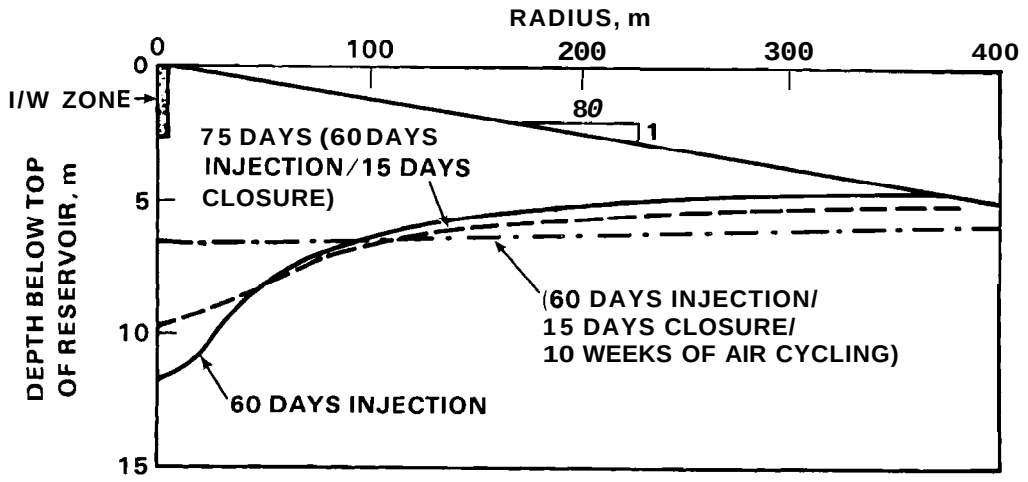

FIGURE 6.5. Equilibration of the 50% Saturation Front - Final Pre-Test Analysis

The process of water migration below the wellbore is further demonstrated by the saturation versus time plots of different weekly cycles, as shown in Figure 6.6. During a withdrawal cycle the saturation increases at a given location. During the subsequent injection cycle, the saturation decreases. The net effect is that water migrates toward the wellbore. Three separate factors are involved although the contribution from each is unknown. First, while the near-wellbore pressure gradients are balanced on both sides of the cycle, the time-integrated force (which is, in essence, the "average" local pressure at each point) is such that net movement is toward the wellbore. Second, the mobility of the water is always imbalanced. The advancing saturation front is fed from below by

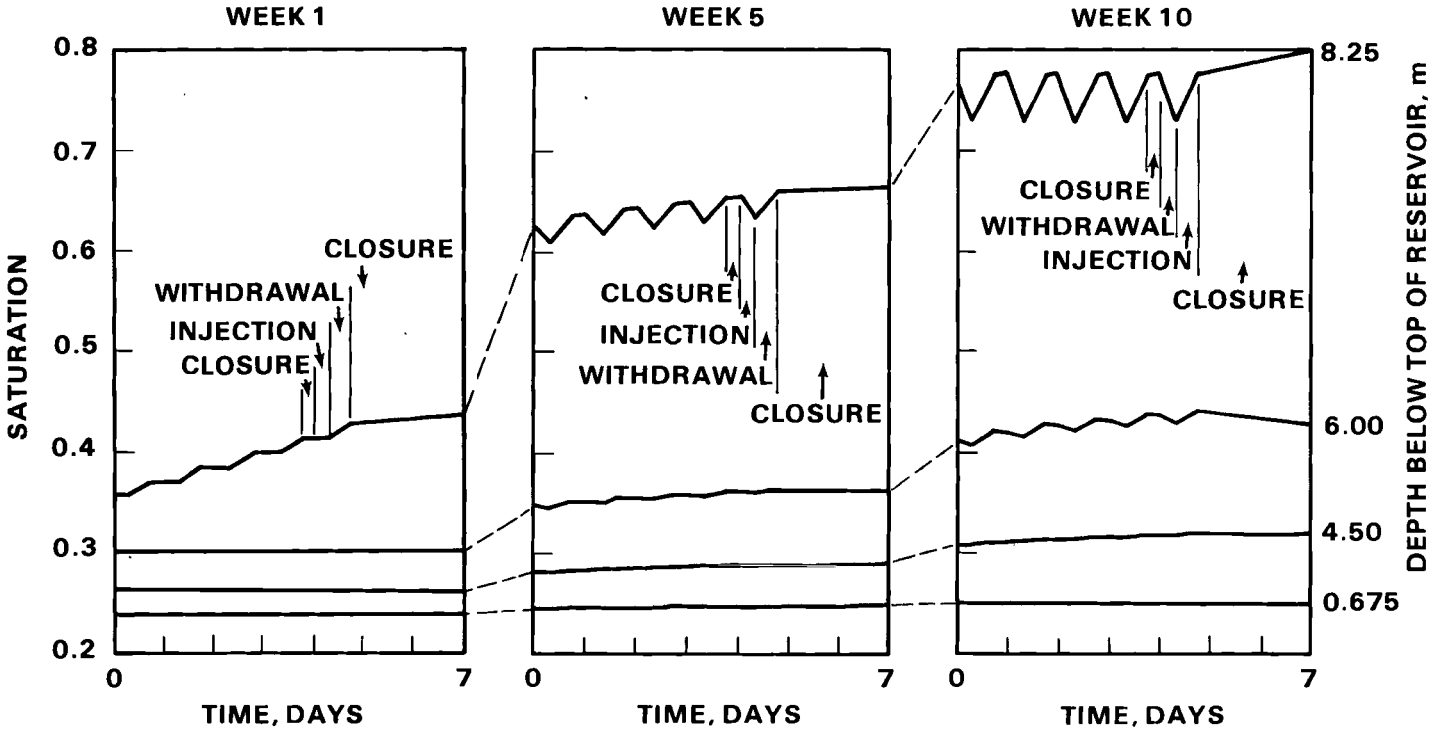

FIGURE 6.6 Saturation Histories for Various Depths Below the Caprock at the Center of the Reservoir - Final Pre-Test Analysis

water of high mobility. The mobility of the receding saturation front depends on the local saturation. The imbalance in mobilities ratchets the front toward the wellbore. Third, the bubble is continuing to equilibrate.

As the saturation increases at a location, the mobility of the water increases. In the time span of one injection/withdrawal cycle the amplitude of the saturation changes wi11 correspondingly increase. This is most notable in Figure 6.6 for the location 8.25 m below the top of the reservoir. The saturation cycles about a nominal value that increases with time.

The evaluation of isothermal air cycling focuses on the behavior of the saturation in the vicinity of the wellbore because of the potential for water production. The other parameter predicted by the two-phase flow model is the pressure. The pressure response is important because of the impact on water production. However, the most important aspect of the pressure response is the impact on the operational efficiency of the reservoir.

The bottomhole pressures at the conclusion of each cycle are shown in Figure 6.7. The difference between the injection and closure pressures is approximately equal to the difference between the withdrawal and closure pressures. Thus, the defined cycle achieves the desired pressure balance. With respect to operational efficiency of the reservoir, it is observed that air is injected at a pressure that is approximately double the recovery pressure. This performance would likely be unacceptable in a commercial CAES facility but the field test was designed for much lower operating pressure than a full-scale facility. The important point is that volume flow rates per unit of sandface surface area are approximately equal, and are also prototypic.

Another result observed in Figure 6.7 is the effect of decay of bubble pressure. At the conclusion of bubble development, the reservoir was taking air at a predicted rate of about 1250 scfm with a defined bottomhole pressure of 290 psia. At the beginning of the air cycling

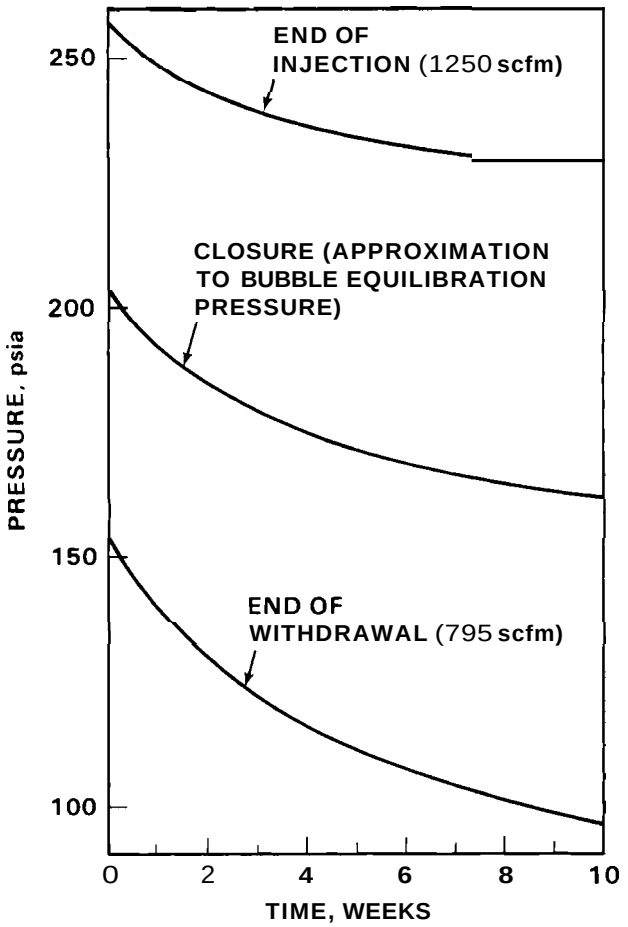

FIGURE 6.7. Bottomhole Pressures During Cycling - Final Pre-Test Analysis

calculation, the reservoir is taking air at 1250 scfm with a bottomhole pressure of 256 psia. This seemingly inconsistent result is due to the equilibration of the bubble during the 15 days of closure that followed bubble development. The bubble pressure decays as the bubble expands against the background hydrostatic pressure. This pressure decay continues during air cycling. After 10 weeks the closure pressure is 161 psia. The closure pressure will never return to the original hydrostatic value. The bubble development has depressed the air-water interface about 10 m below the top of the reservoir. Because the depth of the air-water interface determines the hydrostatic pressure, the equilibrium bubble pressure will be about 11 atm.

7.0 FUTURE WORK

Concurrent modeling is planned in support of the operation of the field test. In this analysis, the key aspect of reservoir modeling will be performance matching. Parameters in the models can be adjusted so that model predictions and reservoir performance are matched. Then the models should be more accurate for use as predictive tools. The success of this approach depends on the use of sound engineering practices in making the adjustments to the model parameters. Otherwise, arbitrary adjustments to these parameters would not, in general, improve the predictive accuracy of the models.

The benefit of performance matching is that it should lead to greater understanding and insight into the geologic properties and performance characteristics of the reservoir. Adjustment of parameters associated with the hydraulic response of the reservoir, such as permeability, relative permeability, and porosity, and those parameters associated with the thermal response of the reservoir, such as conductivity, which lead to more accurate performance predictions, may provide clues to researchers in the field and in the laboratory regarding the value of those parameters as they exist within the reservoir. This interaction may help to resolve expected discrepancies between laboratory data, in-situ data and model predictions. For example, historical precedent indicates in situ hydraulic conductivity is usually higher than core data predicts.

As the field test progresses, the two-dimensional, two-phase isothermal flow model can be used to provide guidance should problems occur related to the flow of fluids in the reservoir. For example, excessive fingering of the initial bubble growth could result in a loss of closure. The model will be useful in determining a new injection schedule and flow rates to reduce the impact of this problem. Also, if water production occurs during the cycle tests, the models will help to define a new cycling schedule and flow rates that will prevent the problem.

The numerical modeling proposed to support the high temperature air cycling will primarily involve the thermal models. Our ability to accurately predict the thermal response of the reservoir will depend on the strength of the coupling between the flow of water and the thermal response. If liquid water continually resaturates the near-wellbore region, the thermal conductance and heat capacity will be altered. The effect of these changes on the thermal response is uncertain because the heat capacity is defined primarily by the host rock and thermal conduction plays a minor role to forced convection for heat transfer in the air storage zone. Also, the rate of resaturation may be slow, thereby precluding the problem. Nevertheless, if the coupling is strong, the current modeling capability will not provide accurate predictions of the performance of the reservoir. Indications of strong coupling would be higher than expected withdrawal humidity and lower temperatures. In this event, a model that combines two-phase flow, thermal effect and phase change would be required.

REFERENCES

PB-KBB, Inc., and David K. Davies and Associates. 1983. Pre-Test Geological and Geochemical Evaluation of the Caprock, St. Peter Sandstone and Formation Fluids - Yakley Field, Pike County, Illinois. PNL-4564, Pacific Northwest Laboratory, Richland, Washington.

Smith, G. C., L. E. Wiles and W. V. Loscutoff. 1979. Numerical Analysis of Temperature and Flow Effects in a Dry, One-Dimensional Aquifer Used for Compressed Air Energy Storage. PNL-2546, Pacific Northwest Laboratory, Richland, Washington.

Wiles, L. E. 1979a. Numerical Analysis of Temperature and Flow Effects in a Dry, Two-Dimensional Porous Media Reservoir Used for Compressed Air Energy Storage. PNL-3047, Pacific Northwest Laboratory, Richland, Washington.

Wiles, L. E. 1979b. The Effects of Water on Compressed Air Energy Storage in Porous Rock Reservoirs. PNL-2869, Pacific Northwest Laboratory, Richland, Washington.

Wiles, L. E., and R. A. McCann. 1981. Water Coning in Porous Media Reservoirs for Compressed Air Energy Storage. PNL-3470, Pacific Northwest Laboratory, Richland, Washington.

DISTRIBUTION

No of Copies

OFFSITE

US Department of Energy
Attn: J. Brogan
Office of Energy Systems Res.
Forrestal Bldg, CE-141 5E-052
Washington, DC 20585

US Department of Energy
Attn: R. A. Dunlop
Div. of Electric Energy Sys.
12 & Pennsylvania
Washington, DC 20585

US Department of Energy
Attn: I. Gyuk
Office of Energy Systems Res.
Forrestal Bldg, CE-141 5E-052
Washington, DC 20585

US Department of Energy
Attn: R. Shivers
Office of Energy Systems Res.
Forrestal Bldg, CE-141 5E-052
Washington, DC 20585

US Department of Energy
Attn: J. H. Swisher
Office of Energy Systems Res.
Forrestal Bldg, CE-141 5E-052
Washington, DC 20585

27 DOE Technical Information Center

Acres American, Inc.
Attn: C. Driggs
The Clark Building
Suite 329
Columbia, MD 21044

No of Copies

Acres American, Inc.
Attn: D. Willett
Liberty Bank Building
Main at Court
Buffalo, NY 14202

Central Illinois Public Service Co.
Attn: A. H. Warnke
Vice President Power Supply
607 East Adams Street
Springfield, IL 62701

Commonwealth Edison Co.
Attn: T. J. Maiman
Sta. Mech. Engr. Dept. Mgr.
36 FN West
PO Box 767
Chicago, IL 60690

C. V. Crow
76 Colorado Drive
Decatur, IL 62526

Electric Power Research Inst.
Attn: R. B. Schainker
3412 Hillview Avenue
PO Box 10412
Palo Alto, CA 94303

Harza Engineering Co.
Attn: A. H. Barber
Director of Marketing
150 S. Wacker Drive
Chicago, IL 60606

Michael J. Hobson
PO Box 820
Columbia, MD 21044

Illinois Power Company
Attn: G. E. Huck
Manager of Planning
500 South 27th St.
Decatur, IL 62525

No of
Copies

Lawrence Livermore Laboratory
Attn: Jesse Yow
PO Box 808
Mail Stop L-202
Livermore, CA 94550

Lawrence Livermore Laboratory
Attn: Tech. Info. Dept, L-3
University of California
PO Box 808
Livermore, CA 94550

Middle South Services
Attn: L. A. Wilson
Advanced Energy Program
Section
Box 6100
New Orleans, LA 70161

PB-KBB, Inc.
Attn: J. Istvan
PO Box 19672
Houston, TX 77024

Potomac Electric Power Co.
Attn: P. E. Schaub
1900 Pennsylvania Ave
Washington, DC 20006

Public Service of Indiana
Attn: T. W. McCafferty
1000 E. Main Street
Plainfield, IN 46168

RE/SPEC Inc.
Attn: A. F. Fossum
PO Box 725
Rapid City, SD 57701

Sandia Laboratories
Attn: William G. Wilson
PO Box 969
Organization 8453
Livermore, CA 94550

No of
Copies

Sandia Laboratories
Attn: R. O. Woods
Organization 4715
Albuquerque, NM 87115

Sargent and Lundy Engineers
Attn: W. C. Walke
Project Manager
55 East Monroe Street
Chicago, IL 60603

Soyland Power Cooperative, Inc.
Attn: Tom Seng
PO Box A1606
Decatur, IL 62525

Tennessee Valley Authority
Attn: A. Betbeze
1150 Chestnut, Tower 2
Chattanooga, TN 37401

Tennessee Valley Authority
Energy Research Section
1360 Commerce Union Bank
Bldg.
Chattanooga, TN 37401

TRW Energy Systems Group
Attn: E. Berman
Technical Library
7600 Colshire Drive
McLean, VA 22101

Union Electric Co.
Attn: H. C. Allen
Vice President
Research & Development
PO Box 149
St. Louis, MO 63166

No of
Copies

United Engineers & Constructors
Attn: E. Sosnowicz
Advanced Eng. Dept. 04U3
30 South 17th
Philadelphia, PA 19101

University of California
Attn: T. L. Brekke
Dept. of Civil Engineering
1847 Yosemite Road
Berkeley, CA 94707

University of Massachusetts
Attn: O. C. Farquhar
Dept. of Geology & Geography
Morrill Science Center
Amherst, MA 01003

University of Michigan
Attn: D. L. Katz
Dept. of Chemical Engineering
2042 E. Engr. Bldg.
Ann Arbor, MI 48109

University of Wisconsin
Attn: H. J. Pincus
Dept. of Geological Sciences
Sabin Hall and Greene Museum
PO Box 413
Milwaukee, WI 53201

Westinghouse Electric Corp.
Attn: W. F. Kobett
CAES Project Manager
Combustion Turbine Sys. Div.
Long Range Develop-Lab 100
PO Box 251
Concordville, PA 19331

Westinghouse Fluid Sys Lab
Attn: J. Y. Baladi
1291 Cumberland Avenue
West Lafayette, IN 47906

No of
Copies

Westinghouse R&D
Attn: D. L. Ayers
1310 Beulah Road
Pittsburg, PA 15235

FOREIGN

Central Electricity Generating Board
Attn: I. Glendenning
6 Georgian Close
Gloucester England
9L4 9DG

ONSITE

DOE Richland Operations Office

H. E. Ransom/D. R. Segna

36 Pacific Northwest Laboratory

R. D. Allen
T. J. Doherty
R. L. Erikson
L. D. Kannberg (20)
R. A. McCann
L. E. Wiles (5)
Technical Information (5)
Publishing Coordination (2)